

## RESEARCH ARTICLE

# Environmental history impacts gene expression during diapause development in the alfalfa leafcutting bee, *Megachile rotundata*

George D. Yocum<sup>1,\*</sup>, Anna K. Childers<sup>1,2</sup>, Joseph P. Rinehart<sup>1</sup>, Arun Rajamohan<sup>1</sup>, Theresa L. Pitts-Singer<sup>3</sup>, Kendra J. Greenlee<sup>4</sup> and Julia H. Bowsher<sup>4</sup>

**ABSTRACT**

Our understanding of the mechanisms controlling insect diapause has increased dramatically with the introduction of global gene expression techniques, such as RNA sequencing (RNA-seq). However, little attention has been given to how ecologically relevant field conditions may affect gene expression during diapause development because previous studies have focused on laboratory-reared and -maintained insects. To determine whether gene expression differs between laboratory and field conditions, prepupae of the alfalfa leafcutting bee, *Megachile rotundata*, entering diapause early or late in the growing season were collected. These two groups were further subdivided in early autumn into laboratory- and field-maintained groups, resulting in four experimental treatments of diapausing prepupae: early and late field, and early and late laboratory. RNA-seq and differential expression analyses were performed on bees from the four treatment groups in November, January, March and May. The number of treatment-specific differentially expressed genes (97 to 1249) outnumbered the number of differentially regulated genes common to all four treatments (14 to 229), indicating that exposure to laboratory or field conditions had a major impact on gene expression during diapause development. Principle component analysis and hierarchical cluster analysis yielded similar grouping of treatments, confirming that the treatments form distinct clusters. Our results support the conclusion that gene expression during the course of diapause development is not a simple ordered sequence, but rather a highly plastic response determined primarily by the environmental history of the individual insect.

**KEY WORDS:** RNA-seq, Dormancy, Omnipotent, Toolkit

**INTRODUCTION**

The ability to survive seasonal environmental changes (e.g. temperature, humidity, nutrient availability) is critical for organisms to complete their life cycles, thereby influencing their ability to occupy certain geographic ranges. Representatives of all animal and plant taxa have evolved some form of dormancy in their life history in response to seasonal changes. Although the terminology differs by taxa (e.g. hibernation, aestivation, diapause), the outcome is the same: organisms alter their physiology to survive harsh conditions.

<sup>1</sup>USDA-ARS Insect Genetics and Biochemistry Research Unit, Fargo, ND 58102, USA. <sup>2</sup>USDA-ARS Bee Research Lab, Beltsville, MD 20705, USA. <sup>3</sup>USDA-ARS Pollinating Insect-Biology, Management, Systematics Research Unit, Logan, UT 84322, USA. <sup>4</sup>Biological Sciences, North Dakota State University, Fargo, ND 58105, USA.

\*Author for correspondence (george.yocum@ars.usda.gov)

ID G.D.Y., 0000-0001-6285-0623

Received 1 November 2017; Accepted 4 May 2018

Within Insecta, the physiological form of dormancy is known as diapause. Most insects that undergo diapause in the temperate zone have a narrow window of a few months from early spring to late summer in which to complete development. Across species, diapause occurs in a diverse range of genetically determined developmental stages, ranging from early blastoderm embryo to adult. However, among the various stages, the diapause phenotype is strikingly similar. Arrested development, cell-cycle arrest, decreased metabolism, increased metabolic reserves and higher stress tolerance all characterize insect diapause (Tauber et al., 1986; Danks, 1987; Denlinger, 2002).

Prior to the initiation of diapause, there is a distinct physiological stage known as the pre-diapause phase. During the pre-diapause phase, the insect receives the environmental cues forewarning of future adverse environmental conditions and makes preparations for entering diapause. These preparations may include accumulation of metabolic reserves, migration, or selection of an environmentally buffered site to spend the duration of the adverse season. After the pre-diapause period, the insect enters into diapause. Diapause is further subdivided into three phases, initiation, maintenance and termination. Transition through these phases is known as diapause development (Koštál, 2006). During the initiation phase, direct development stops and metabolism is suppressed. The maintenance phase is characterized by endogenous blocking of direct development even under conditions favorable for development. During the termination phase, control of direct development is switched from being endogenously to exogenously controlled, i.e. from hormonally to thermally controlled. Diapause commonly terminates before the period of adverse environmental conditions have ended, whereupon the insect enters into a period referred to as post-diapause quiescence. During this period, an insect retains many aspects of diapause such as decreased metabolism and increased tolerance to environmental stress, but will slowly regain the ability for normal development as environmental factors return to more favorable conditions. Although these divisions of diapause development are useful for referring to a specific suite of physiological functions, they are also somewhat misleading, because diapause development does not abruptly shift from one phase to another but instead progresses along a continuum (Sawer et al., 1993; Koštál, 2006; Koštál et al., 2017). Another factor impeding the development of a comprehensive understanding of diapause physiology is that currently the majority of our understanding of diapause is derived from laboratory investigations. But insects diapausing under field conditions are subjected to a wide range of environmental factors that vary within and between seasons in both duration and severity. This raises the question as to the degree to which environmental factors shape diapause physiology (as reflected in the transcriptome response) over the course of overwintering.

Global gene expression techniques have greatly expanded our ability to understand the molecular regulation of diapause (Emerson

et al., 2010; Ragland et al., 2010, 2011; Poelchau et al., 2011, 2013a,b; Gong et al., 2013; Dong et al., 2014; Huang et al., 2015; Qi et al., 2015; Yocom et al., 2015; Hao et al., 2016; Kang et al., 2016; Meyers et al., 2016; Koštál et al., 2017). Observed similarities in specific gene expression patterns between species has led a number of research teams to propose the existence of a conserved ‘diapause genetic toolkit’ (Ragland et al., 2010; Poelchau et al., 2013a; Huestis and Lehmann, 2014; Amsalem et al., 2015; Yocom et al., 2015; Ragland and Keep, 2017). Others have argued that if a diapause toolkit exists, it is conserved at the pathway level and not in expression patterns of individual transcripts (Ragland et al., 2010; Koštál et al., 2017). A significant challenge in testing these hypotheses is that environmental signals modify the physiological and chronological progression of diapause (Koštál, 2006). If the physiological processes underlying the phases of diapause development are impacted by the interaction of environmental factors, gene expression patterns should also reflect this complexity, thereby compounding the technical challenge of identifying any possible diapause toolkit.

The alfalfa leafcutting bee, *Megachile rotundata* (Fabricius 1787) (Hymenoptera: Megachilidae), is an intensely managed solitary bee used as the primary pollinator of alfalfa for seed production in North America (Pitts-Singer and Cane, 2011). Under agricultural management, *M. rotundata* adults emerge from leaf-wrapped cocoons in late June or early July, after spending the winter as prepupae. Each female constructs a series of brood cells in artificial nest blocks consisting of linear cavities. Once a cell is provisioned with pollen and nectar, the female will lay a single egg, seal the cell and then start to construct the next cell. The egg hatches, and the larva eats its provision mass, completes development within the cell, and either enters diapause as a prepupa or continues development to the adult stage for summer emergence (Krunic, 1972; Hobbs and Richards, 1979; Kemp and Bosch, 2001). The progeny of summer-emerging adults (second generation) are generated in the late summer and develop to the diapausing prepupal stage. These two brood cohorts (those entering diapause in June/July and those entering diapause in August/September) have very different thermal histories. The prepupae that enter diapause early in the field season are subjected to summer temperatures, whereas those that diapause late in the season experience only autumn temperatures before the onset of winter.

The objective of this investigation was to determine the degree to which environmental history impacts gene expression during the course of diapause development in *M. rotundata*. To achieve our objective, early and late diapausing prepupae were collected, and in the late autumn, the early and late diapausing groups were further separated into two groups: one that remained outdoors in ambient conditions and one that was maintained under constantly cool laboratory conditions. RNA sequencing (RNA-seq) and differential expression analyses were performed on all four treatment groups sampled in the autumn, winter and the following spring (March and May).

## MATERIALS AND METHODS

### Insects

The *M. rotundata* that nested in Utah in the summer of 2009 originated from brood reared in commercial alfalfa fields in Wyoming, USA; the bees were then purchased by a Utah alfalfa seed grower for pollination in summer. Bees were incubated in an on-farm facility and released as adults on 26 June 2010 into a Utah alfalfa field ( $41^{\circ}47'37.04''N$ ;  $112^{\circ}8'18.35''W$ ). Polystyrene nesting blocks (Beaver Plastics, Ltd, Alberta, Canada) had been placed in

field domiciles for bee nesting (Pitts-Singer and Cane, 2011), and in several of the blocks, paper straws were inserted into holes as cavity liners. Twice weekly, straws that had been filled with nest cells were removed from the holes and empty straws were inserted into vacated holes. Straws were brought into the USDA-ARS Pollinating Insects Research Unit (Logan, UT, USA), and the date when straws were recovered was recorded. Straws were aligned and adhered to plastic boards to secure the straws for placement into a digital X-ray machine (Faxitron 43804N, Faxitron Biophysics, Tucson, AZ, USA) and to align digital images with the actual nest cells. Nests on boards were then stored outdoors in an open shelter (protected from direct sunlight and rain), where the temperature was recorded with a HOBO Datalogger (Fig. S1; Onset Computer Corp., Bourne, MA, USA). Nests were X-radiographed weekly throughout the summer to determine the developmental stages of the bees still in their nest cells. Development to the pupal stage indicated that those individual bees had averted diapause and were destined to metamorphose to adulthood without spending the winter in the prepupal (diapausing) stage.

For this experiment, bees that entered diapause early and late in the nesting season were needed (Fig. 1). Early season nests were designated as those from straws pulled between 30 June and 19 July 2010. Late season nests were designated as those pulled on 1 September 2010. Based on the female bee’s lifespan of 7 to 8 weeks, the early season diapausing progeny were generated by the adults of the 2009 brood, but the late season nests most likely were generated by non-diapausing bees that emerged during early summer 2010 (Pitts-Singer and Cane, 2011). For early season nests, only those in which all cells contained diapausing prepupae were used. Bee cells were dissected from nests in September 2010, transferred to individual gelatin capsules, and tracked using unique identifiers. Early and late season groups were divided into two overwintering management groups: (1) laboratory bees, overwintered in the laboratory according to standard commercial storage practices; and (2) field bees, overwintered outside at ambient temperatures while shielded from direct sunlight or rain. Therefore, four treatment groups were designated: (1) early season, field managed (EField), (2) early season, laboratory managed (ELab), (3) late season, field managed (LField) and (4) late season, laboratory managed (LLab). To assure that bees assigned to treatments were genetically diverse, prepupae from the same nest were distributed between field and laboratory treatments for both the early and late diapausing groups. All individual bee cells were maintained outdoors at ambient temperature until 22 October 2010. On that date, early and late season bee cells that were designated for laboratory-managed groups were moved to an incubator held at a constant  $16^{\circ}\text{C}$ , and on 1 November 2010 were placed into an environmental chamber maintained at  $4\text{--}5^{\circ}\text{C}$  and in darkness. Temperature continued to be recorded outdoors for the duration of the study (Fig. S1). Monthly from October 2010 to June 2011, we removed prepupae for future RNA extraction from each of the four treatment groups. Twenty whole prepupae per treatment were excised from their cocoons, placed individually into Eppendorf tubes, flash-frozen in liquid nitrogen and stored at  $-80^{\circ}\text{C}$ .

### RNA

Samples from four time points (November, January, March and May) were chosen to span the diapause maintenance (November), termination (January) and post-diapause quiescent stages (March and May) of development (Johansen and Eves, 1973; Yocom et al., 2006). RNA was extracted from three prepupae haphazardly chosen

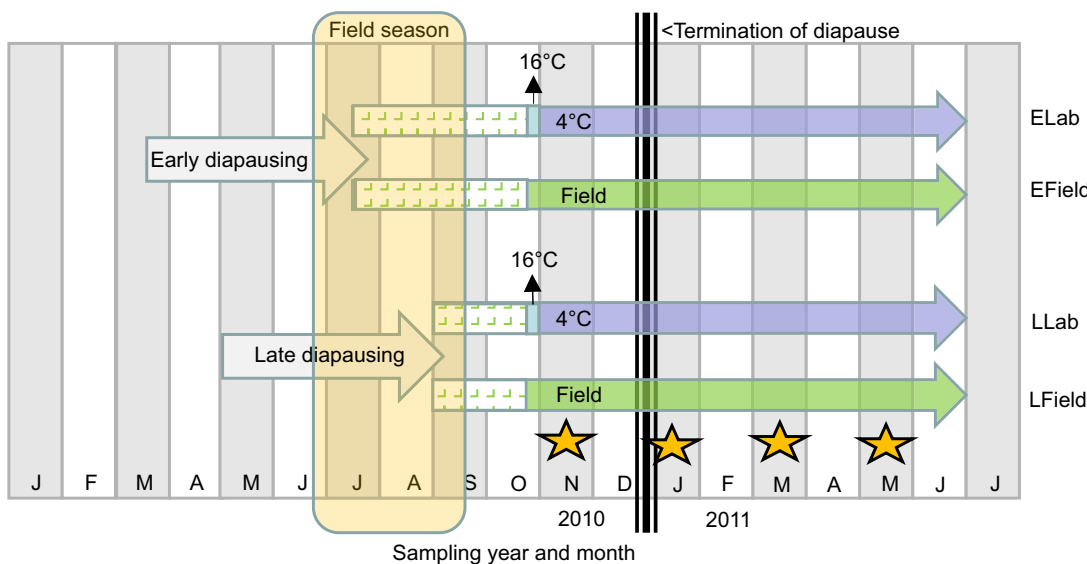


**Fig. 1. Schematics of experimental design.** *Megachile rotundata* diapausing prepupae were collected early and late in the nesting season. All diapausing prepupae were maintained under field conditions until October when the prepupae from each group [early (E) and late (L)] were further subdivided into laboratory or field management types resulting in four treatment groups: early laboratory, late laboratory, early field and late field. RNA-seq libraries were constructed from samples taken from each group in November, January, March and May (stars) for paired-end Illumina sequencing.

from samples for each of the four treatments and months (48 total samples). Bees were ground in liquid nitrogen, combined with 1 ml of TRIzol (Invitrogen, Life Technologies, Grand Island, NY, USA), and extracted according to the manufacturer's instructions. The isolated RNA pellets were stored under absolute ethyl alcohol at  $-80^{\circ}\text{C}$  until needed.

#### Illumina sequencing

Illumina sequencing was carried out by the Georgia Genomic Facility of the University of Georgia. Stranded Illumina libraries were constructed using the TruSeq RNA kit (Illumina Inc., San Diego, CA, USA). Two lanes of 100 bp paired-end sequencing were performed on each RNA sample using an Illumina HiSeq 2000 sequencer.

#### RNA-seq quality trimming, assembly and differential gene expression analysis

Raw 100 bp Illumina reads were quality trimmed using a Phred quality score cut-off of 19 with DynamicTrim (SolexaQA\_v.2.2), and only those reads with a minimum length of 50 bp were retained using LengthSort (SolexaQA\_v.2.2) (Cox et al., 2010).

Transcript assembly and differential gene expression analyses were carried out using the Tuxedo Suite (Trapnell et al., 2012). Based on an Agilent 2100 Bioanalyzer report (Agilent Technologies, Santa Clara, CA, USA) on the sequenced libraries, we calculated the `-mate-inner-dist` and the `-mate-std-dev` parameters for TopHat2 (v2.0.10) (Kim et al., 2013) transcript alignment to the Mrot\_1.0 genome assembly (Kapheim et al., 2015). The inner distance between the mate pairs was calculated to be 0 bp by subtracting the adapter length ( $\sim 125$  bp) and the length of the paired-end reads (200 bp) from the average size of the Illumina libraries (324 bp). Because the size distribution of the library had a right skew, we used a conservative standard deviation of 24 bp, one-third the calculated standard deviation of the library. In addition, because the libraries were stranded, we used the library-type `fr-first` strand parameter in TopHat2. Data from both Illumina lanes for each sample were pooled. Next, Cufflinks (v2.1.1;

<http://cole-trapnell-lab.github.io/cufflinks/>) was used to generate transcripts from the TopHat2 output for each sample. Then all transcripts were combined using Cuffmerge (v1.0.0) to generate a single reference transcript assembly. This reference transcript assembly and each sample's individual output from TopHat2 was input into Cuffdiff (v2.1.1), which performed pairwise comparisons between all 48 samples for differential gene expression analyses. The completeness of the transcript assembly was estimated using BUSCO software (Benchmarking Universal Single-Copy Orthologs; v1.1b1) (Simão et al., 2015) with the arthropod reference gene set (released December 2014, contained 2675 genes).

#### Assignment of gene descriptions

In order to minimize uninformative annotations (such as 'hypothetical protein'), we conducted three rounds of BLAST. In the first round, NCBI's BLASTX (version 2.2.30+) (Camacho et al., 2009) was used to align all transcripts assembled by Cufflinks to RefSeq proteins (downloaded 29 January 2015 with 21,778 entries) from *Apis mellifera*, the most closely related well-annotated species, keeping only the best hit with an E-value cut-off of  $1 \times 10^{-6}$ . Any transcripts with a poor alignment (hypothetical, uncharacterized or unnamed proteins) or without an alignment were aligned to NCBI's nr database (<ftp://ftp.ncbi.nlm.nih.gov/blast/db/>; downloaded 29 January 2015) using an E-value cut-off of  $1 \times 10^{-6}$  and the `negative_gilist` option to exclude hypothetical, uncharacterized or unnamed proteins (GI numbers downloaded 13 February 2015). Finally, for those remaining unidentified transcripts, a third round of BLAST was performed against the full nr database using an E-value cut-off of  $1 \times 10^{-6}$ , which allowed less informative descriptions (hypothetical, uncharacterized or unnamed proteins) in order to preserve knowledge of known homologs.

#### GO term and KEGG pathway enrichment analysis

Gene ontology (GO) terms were assigned using Blast2GO Pro (Conesa et al., 2005). KEGG (Kyoto Encyclopedia of Genes and Genomes) pathways (December 2015 release; Kanehisa and Goto, 2000) were assigned using the DAVID Knowledgebase (DAVID

6.8; Huang et al., 2009) based on the protein GI identifiers obtained from protein alignments using BLASTX (see above) with all species used for annotations. Because some genes had multiple transcripts, identifiers from proteins aligned to all transcripts for a given gene were included in the analysis. Genes expressed over the average threshold of all genes in the hierarchical cluster analysis (see below) that determined the formation of the primary clusters were used in gene category over-representation analyses using the GOseq package (version 1.18.0) (Young et al., 2010) in R (version 3.1.3, <http://www.R-project.org/>). Enrichment analyses were run on the gene level to remove bias owing to variable numbers of transcripts for each gene. Each gene's length was taken as the median of the lengths of all transcripts. All GO terms and KEGG pathways associated with any of the gene's transcripts were mapped to the gene feature. A 0.05 false discovery rate (FDR) cut-off (Benjamini and Hochberg, 1995) was applied for multiple testing correction.

### Statistical analysis and Venn diagrams

Principle component analysis (PCA) and hierarchical cluster analysis were carried out using JMP (v. 12.0, SAS Institute, 2015, Cary, NC, USA). The data, consisting of 13,564 genes and 16 treatment groups (described above), were log-transformed and first subjected to PCA. Following the PCA, hierarchical cluster analysis by both Ward- and average-linkage methods was performed on normal standardized and robustly standardized data (Eisen et al., 1998). Satisfactory cluster separation by treatment variables was noted with the Ward-linkage method and normal standardization. The effects of overwintering site (laboratory or field), month (month the samples were collected; November, January, March or May) and timing of diapause initiation (early or late) noted in the hierarchical cluster analysis were further confirmed using linear modeling in JMP Genomics 8.2 (SAS Institute). Standardized and log-transformed cluster data derived from the cluster analysis were subject to ANOVA in JMP Genomics. Venn diagrams were generated using Venny 2.0 (<http://bioinfogp.cnb.csic.es/tools/venny/index.html>).

## RESULTS

### Transcriptome assembly and annotation

Sequencing resulted in a total of 409,970,200 raw reads for all 48 samples, with an average of 8,541,045 raw reads per sample. On average, 14% of the raw reads for each sample were discarded in the quality trimming stage. Quality-trimmed RNA-seq reads had an average 87.8% overall and 84.3% concordant pair alignment rate to the *M. rotundata* genome assembly (Table S1). Using the data from all samples, we assembled a transcriptome representing 13,566 gene loci with 50,081 total transcripts (isoforms). Based on the BUSCO transcriptome completeness assessment, more than 92% of *M. rotundata* protein-coding genes were transcribed during the developmental periods evaluated (86.8% of expected genes were complete, another 5.9% were fragmented and 7.3% were missing).

The staged BLAST approach resulted in 85.7% of the transcripts being assigned a descriptive annotation (the description was not derived from hypothetical, uncharacterized and unnamed proteins) and another 1.8% of the transcripts had similarity to hypothetical proteins.

Blast2GO associated a total of 81,545 GO terms with 29,387 of the transcripts (58.7%), such that at least one of the transcripts from 5847 of the genes (43.1%) had a GO annotation. DAVID associated a total of 3372 KEGG pathways with 7165 transcripts (14.3%), such that at least one of the transcripts from 1623 of the genes (12%) was associated with a KEGG pathway. Within the full

data set, 2066 unique GO terms and 131 unique KEGG pathways are represented.

### Differential gene expression analysis

With the current experimental design, two types of comparisons could be carried out. We first compared all biologically relevant combinations within each sampling month (EField versus LField, ELab versus LLab, ELab versus EField, and LLab versus LField) (Table S2). The number of differentially regulated genes varied from as low as 104 upregulated genes in the November ELab versus LLab comparison to 1273 downregulated genes in the May ELab versus EField comparison. The percentage of differentially regulated genes varied from 0.77 to 9.39%, with the largest differences seen in the May comparisons.

The second type of comparison conducted was a sequential, month-to-month analysis to characterize gene expression during diapause development by treatment. Within each treatment, the November, January and March samples were used as the reference for determining differentially regulated genes in the succeeding months. This resulted in three comparisons with November as the reference group (January, March and May), two for January (March and May) and one for March (May). In these six between-month comparisons, the total number of differentially regulated genes for the combined four treatments varied from 722 (January to March comparison) to 2515 (November to May comparison) (Table S2). Venn diagrams of these between-month differentially regulated genes revealed that only 0.9% (March to May) to 14.5% (January to March) of the differentially regulated genes were shared between all four treatments (Figs 2 and 3). Considering all of the comparisons, a total of 566 genes (406 non-redundant) were shared between all four treatments, and only 130 of these genes were common to more than one comparison (Table S3). The total number of treatment-specific genes (upregulated plus downregulated) ranged from 97 in the November to January EField comparison to 1249 in the March to May EField comparison.

### Principal component analysis

Principal component analysis was carried out to determine the relationship between the 16 experimental groups (four treatments at each of four time points) (Fig. 4A). The first two principle components (PCs) explained 89.74% of the total variance. PC1 accounted for 62.53% of the total variance, was explained by the months November, January and March, and encompassed the experimental groups including ENovField, EJanLab, LJanLab, LJanField, EMarLab, EMarField and LMayLab. PC2 accounted for 27.21% of the total variance, was explained by the experimental groups ENovLab, LNovLab, LNovField and EMayField. These four treatments form two distinct clusters: the November laboratory cluster (ENovLab and LNovLab) and the May field cluster (EMayField and LMayField). Both of these clusters were negatively correlated with the primary cluster on the PC1 axis. The May field cluster was negatively correlated with each of the other clusters on the PC2 axis.

### ANOVA of differentially regulated genes

To determine which factor(s) had a statistically significant impact on gene expression, ANOVA was performed (Table 1). Over the course of diapause development, the overwintering site (field or laboratory) and month the samples were collected had a significant impact on gene expression ( $F_{1,1760}=233.71, P=0.00$  and  $F_{3,1760}=44.32, P=0.00$ , respectively). But, timing of diapause initiation (early or late) was not significant ( $F_{1,1760}=0.03, P=0.87$ ). The interaction term for the

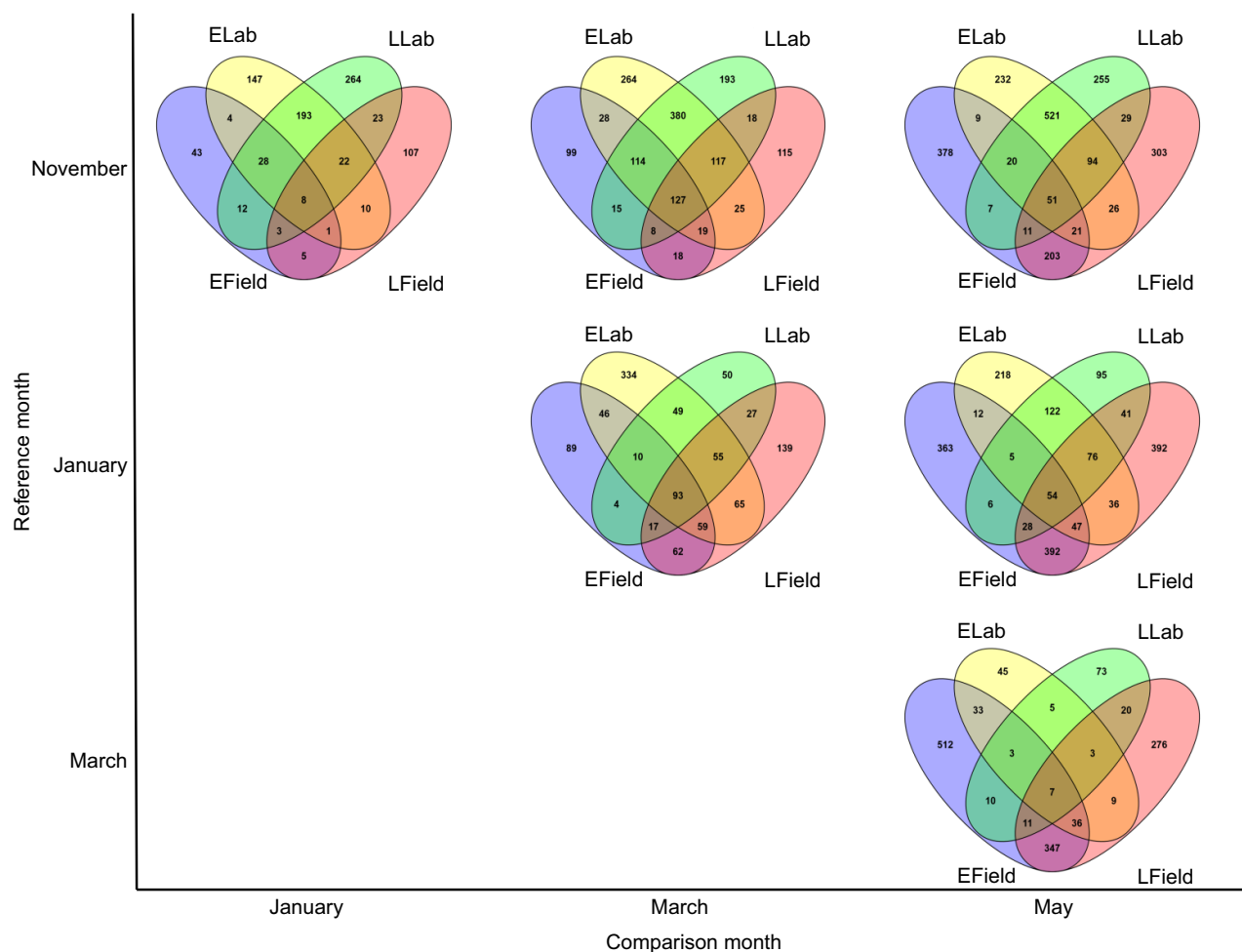


**Fig. 2. Overlap of upregulated genes.** Within each row and treatment group, gene expression status is relative to the reference month (November, January or March). Venn diagrams are labeled according to the timing that the prepupae entered diapause, early (E) or late (L) in the nesting season and the overwintering site, field (Field) or laboratory (Lab).

overwintering site by month was significant ( $F_{3,1760}=45.30, P=0.00$ ). No interactions that incorporated the timing of diapause initiation were significant (timing  $\times$  month,  $F_{3,1760}=0.04, P=0.99$ ; timing  $\times$  overwintering site,  $F_{1,1760}=0.04, P=0.85$ ; or timing  $\times$  month  $\times$  overwintering site,  $F_{3,1760}=0.00, P=1.0$ ). The adjusted  $R^2$  value for the analysis was 0.2432.

#### Hierarchical cluster analysis of global gene expression

Hierarchical cluster analysis of the expression level of all the genes yielded two superclusters and nine clades. Supercluster 1 consisted of clades comprising the treatments separated by PC2, ENovLab, LNovLab (1.1) and EMayField, LMayField (1.2) (Fig. 4B). An alternate method for visualizing results from hierarchical cluster analysis that includes distance comparisons is the constellation plot (Fig. 4C). The constellation plot of the present cluster analysis yielded two main observations. The first is a high degree of similarity between the May field (early and late) samples with the November laboratory (early and late) samples. The second observation is that the most dissimilar within-month comparison is the November laboratory (early and late) versus the November field (early and late) samples. These two treatment groupings are situated at opposite ends of the constellation plot, indicating a low level of similarity.

#### Gene ontology and KEGG pathway enrichment

The grouping of ENovLab, LNovLab, EMayField and LMayField into supercluster 1 was an unexpected result from the hierarchical cluster analysis. To determine the physiological basis for this grouping, enrichment analysis was carried out. Genes contributing to the formation of supercluster 1 were enriched for 17 overrepresented GO terms and three KEGG pathways. The majority of the enriched GO terms were associated with ribosomal function, translation and ATP synthesis (Table S4), whereas the KEGG pathways included the oxidative phosphorylation, proteasome and ribosome pathways (Table S4). There were no under-represented GO terms or KEGG pathways associated with supercluster 1.

#### November field versus November laboratory differentially regulated genes

Because the November field and laboratory samples were the least similar based on the results of the constellation plot, we compared gene expression levels between these groups to determine the physiological basis for this result. Four comparisons were carried out: LNovField to LNovLab, LNovField to ENovLab, ENovField to LNovLab, and ENovField to ENovLab. Only those genes that were differentially regulated in the same direction in all comparisons were kept for further consideration. Between the November field samples

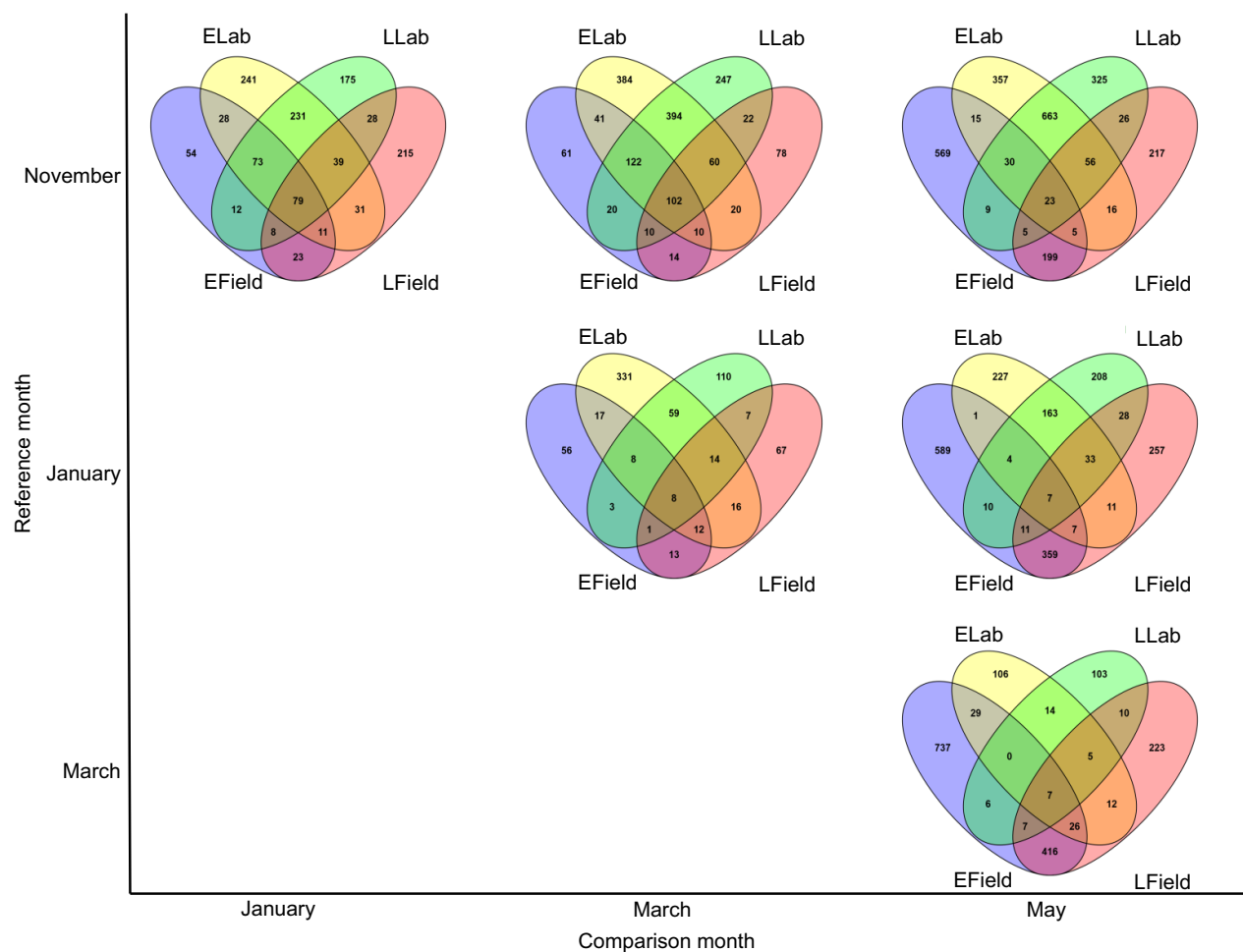


**Fig. 3. Overlap of downregulated genes.** Within each row and treatment group, gene expression status is relative to the reference month (November, January or March). Venn diagrams are labeled according to the timing that the prepupae entered diapause, early (E) or late (L) in the nesting season and the overwintering site, field (Field) or laboratory (Lab).

and the November laboratory samples, 107 genes were differentially regulated (Table S2). Within the differentially regulated genes, 74 were upregulated in the field samples. Notably, five of these differentially regulated genes were regulatory genes: cyclin-dependent kinase 1 (*CDK1*), anaphase-promoting complex subunit 15 (*ANAPC15*), Cactus (*IkB*), Bicaudal C (*BicC*) and *Samui*.

## DISCUSSION

The goal of this study was to determine whether environmental history affects gene expression over the course of diapause development. We concentrated on two environmental factors, the timing of diapause initiation (early and late) and overwintering conditions (constant or fluctuating temperatures), to address this question. Both of these factors had a major impact on the gene expression patterns. The differences in gene expression patterns between the four treatment groups in both the within- and between-months comparisons strongly suggest that these bees were physiologically different. The impact of environmental history on insect physiology during the course of diapause development presents a significant challenge for identifying those genes that make up a possible ‘genetic toolkit’.

### Influence of early versus late diapause initiation

The analysis of the effect of timing of entering diapause (early or late) on gene expression gave conflicting results. Time was an

insignificant factor in our ANOVA model and the PCA and hierarchical cluster analyses failed to clearly separate the early and late treatments. But, timing of entering diapause clearly impacted gene expression patterns over the course of diapause development (Figs 2 and 3). The shift in gene expression patterns between the early and late samples had occurred by the time of the November sampling. We would argue that although statistically insignificant, timing is not biologically irrelevant. However, based on the ANOVA, PCA and hierarchical cluster analyses, the overwintering conditions (field versus laboratory) and month of sampling are the primary drivers for the physiological separation between the various treatment groups. Yet, these two factors only explained 24% of total variance in the ANOVA model, indicating that there are other unaccounted-for factor(s) impacting gene expression during diapause.

### Impact of field versus laboratory overwintering conditions

Transcriptomes of diapausing *M. rotundata* diverged quickly when transferred from a thermally fluctuating field environment to the constant environment of the laboratory. By the time the November samples were collected, the laboratory samples had been transferred from the field to 16°C for 9 days. During this same period, the field bees were exposed to a range of temperatures (3.7–14.8°C) with a mean of 7.7°C (Fig. S1). The most striking result of the PCA and

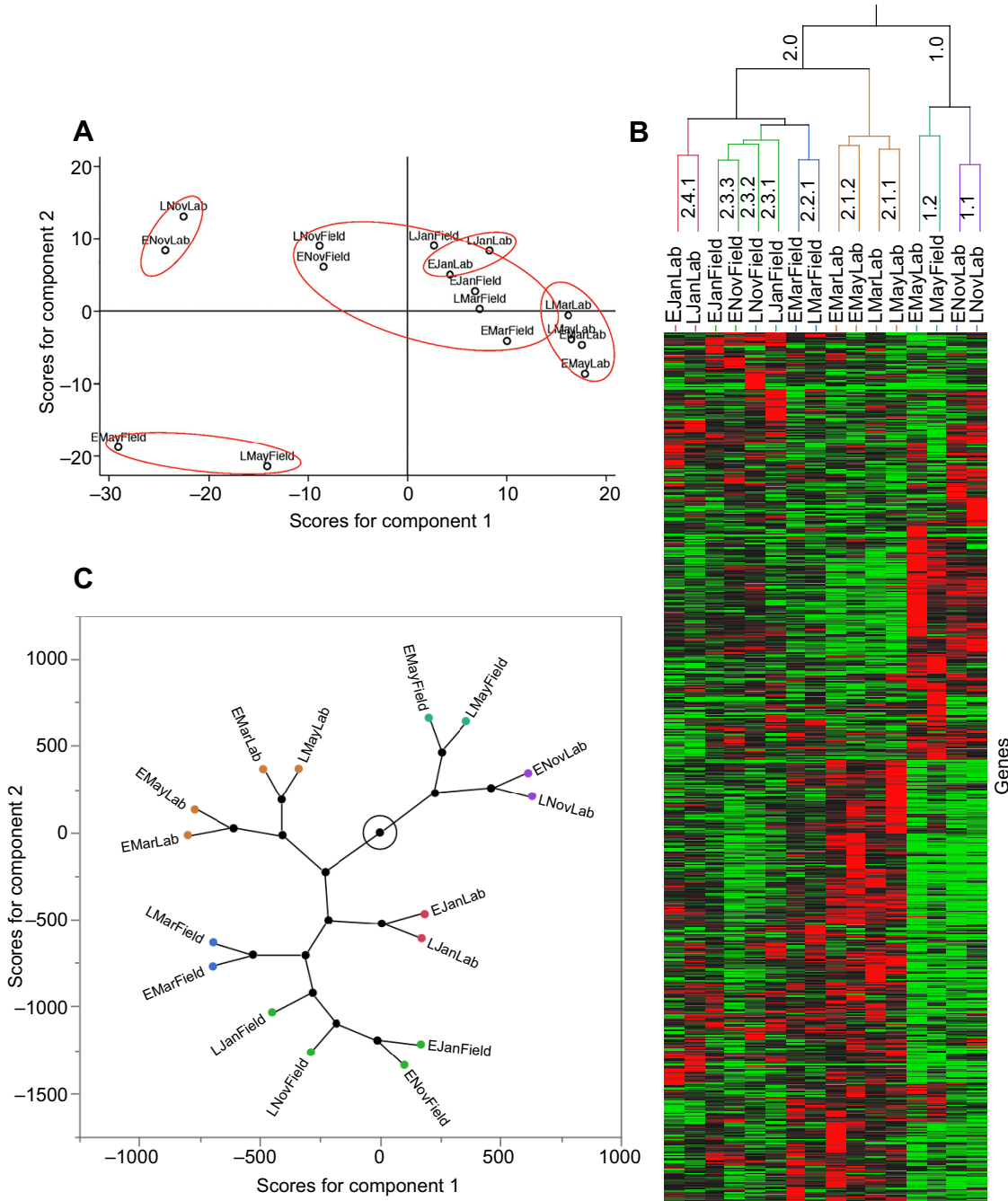


**Fig. 4. Multivariate analysis of the impact of environmental history on diapause development in *Megachile rotundata*.** The 16 different treatments are labeled according to the timing that the prepupae entered diapause, early (E) or late (L) in the nesting season, and the overwintering site, field (Field) or laboratory (Lab), as well as the month sampled. Illumina sequencing determined the expression levels for a total of 13,566 genes. The normalized gene expression levels for each gene were employed for the multivariate analysis: principle component analysis score plot (A), geometric dendrogram (B) and constellation plot (C). Constellation plots use the groups' constellation coordinates and distance calculations to give a relative measurement of similarity between the groups. The greater the distance, the less similar the groups. The node circled in the constellation plot is the root node.

hierarchical cluster analyses was the supercluster 1 grouping of the November early and late laboratory treatments with the May early and late field treatments (Fig. 4B). This supercluster was characterized by overrepresentation of genes associated with GO terms and KEGG pathways for increased protein synthesis (ribosome, translation and ATP synthesis). Because bees in the May field treatments experienced temperature pulses above the developmental threshold for *M. rotundata* ( $\sim 16\text{--}18^\circ\text{C}$ ) (O'Neill

et al., 2011), they would be expected to have resumed direct development. Therefore, the increase in protein synthesis is reasonable. The indication of a higher level of protein synthesis in the November laboratory treatments is somewhat more perplexing. Like the May field samples, the higher level of protein synthesis in the November laboratory samples may be due to the elevated temperature ( $16^\circ\text{C}$ ) relative to the temperatures experienced by the field prepupae during this same time period. Nevertheless, it

**Table 1.** ANOVA results of *Megachile rotundata* diapause regulated genes

Source	Partial SS	d.f.	MS	F	Prob>F
Model	1249.28	15	83.29	39.03	0.00
Timing <sup>a</sup>	0.05	1	0.05	0.03	0.87
Month <sup>b</sup>	283.74	3	94.58	44.32	0.00
Location <sup>c</sup>	498.73	1	498.73	233.71	0.00
Timing×Month	0.24	3	0.08	0.04	0.99
Timing×Location	0.08	1	0.08	0.04	0.85
Month×Location	290.03	3	96.68	45.30	0.00
Timing×Month×Location	0.11	3	0.00	0.00	1.00
Residual	3755.82	1760	2.13		
Total	5005.10	1775	2.82		

<sup>a</sup>Timing of diapause initiation (early or late).

<sup>b</sup>Month samples were collected (November, January, March or May).

<sup>c</sup>Location of the overwintering site (laboratory or field).

indicates that the environmental history of the November laboratory treatments made this group physiologically distinct.

Another striking result was the degree of dissimilarity between the November laboratory (early and late) and November field (early and late) treatments, best seen in the constellation plot (Fig. 4C). Because the November treatments were at the start of the experiment, we expected that these groups would have a high degree of similarity. Yet, the November laboratory and field treatments are situated on the opposite ends of the plot, indicating a low level of similarity relative to the other treatment groups. Examination of the differentially regulated genes between the field and laboratory November samples revealed a shift in key regulatory genes associated with diapause.

A universal hallmark of insect diapause is cell cycle arrest (Nakagaki et al., 1991; Tammaro and Denlinger, 1998; Koštál et al., 2009; Poelchau et al., 2011, 2013a; Yocum et al., 2015; Ragland and Kepp, 2017). Comparison between the November field and laboratory samples found evidence for differences in this key trait, with the cell cycle regulatory genes *CDK1*, *ANAPC15* and *ING3* being upregulated in the laboratory samples. *CDK1* targets approximately 75 genes that control various aspects of the cell cycle, and therefore is an essential gene for the progression of the cell cycle (Malumbres and Barbacid, 2009; Enserink and Kolodner, 2010). The anaphase-promoting complex (*ANAPC15*) is essential for the initiation of DNA replication and sister chromatid separation during cell proliferation (Peters, 2006). The ING family of tumor suppressor proteins are highly conserved across taxa and are involved in the regulation of cell cycle arrest, DNA repair, regulation of gene expression, apoptosis and chromatin remodeling (Campos et al., 2004; Doyon et al., 2006; Cole and Jones, 2008; Aguiissa-Touré et al., 2011). *ING3* in particular is known primarily to function in cell cycle arrest, apoptosis and chromatin remodeling. However, in prostate cancer, *ING3* has been shown to promote cell proliferation, which demonstrates that it is environmentally dependent in cell cycle progression (Nabbi et al., 2017). Regardless of the physiological role of *CDK1*, *ANAPC15* and *ING3* in diapause, their differential expression lends more evidence to the physiological distinctions between the November field and laboratory samples.

Further evidence for differences in cell cycle regulation between the November field and laboratory samples is indicated by the differential regulation in key regulatory pathways. *IkB*, an inhibitor of the NF-κB pathway (Belvin et al., 1995; Ray et al., 1995), and *BicC*, an inhibitor of the wnt pathway (Maisonneuve et al., 2009; Park et al., 2016), are both upregulated in the field samples relative to laboratory, indicating that both the NF-κB and wnt pathways are

being downregulated in the field bees. Inhibiting either the NF-κB or the wnt pathway would decrease progression through the cell cycle (Joyce et al., 2001; Niehrs and Acebron, 2012). Taken together, these results indicate that the cell cycle is being differentially regulated between the laboratory and field samples.

Of the differentially regulated genes we identified, the most thoroughly studied diapause-related gene is *Samui*, which was upregulated in the November field samples. *Samui* is a cold-induced gene that has been isolated in *Bombyx mori* (Moribe et al., 2001). *Samui* is a member of the BAG family of proteins (Moribe et al., 2001), which are highly conserved and have been demonstrated to interact with signaling pathways and molecular chaperones (Doong et al., 2002; Kabbage and Dickman, 2008). Based on the correlation between the temperature-dependent profile of *Samui* expression and termination of diapause, as well as the timing of *Samui* expression early during low temperature exposure, it was proposed that *Samui* serves as a trigger for terminating diapause in *B. mori* (Moribe et al., 2001, 2002). The upregulation of *Samui* in the November field samples may indicate that the process of diapause termination has started in these samples.

#### Thermal history is a confounding factor in diapause transcriptome investigations

The present study considered only two factors: (1) the timing of entering diapause and (2) the overwintering conditions. We found a wide variation in gene expression patterns between the four treatments at each of the four time points examined. The simplest hypothesis for this observation is that the treatments desynchronized the bees' diapause development, resulting in the observation of different expression patterns for each group. As such, this hypothesis presupposes that diapause development is a fixed genetic pathway following a single order of gene expression patterns. A counter argument to desynchronization is that chilling of diapausing *M. rotundata* prepupae typically synchronizes adult emergence. Previous work has shown that chilling prepupae for 7 months (the same duration as the current May samples) decreased the emergence interval to 12 days from approximately 11 months when no chilling occurred (Johansen and Eves, 1973). Therefore, because all the bees experienced several months of chilling in this study, it can be reasonably argued that if *M. rotundata* diapause was driven by a single fixed pathway, the bee physiology should have been more similar as diapause progressed compared with the dissimilarity we found. Given these data, we propose an alternate hypothesis: that there are multiple genetic profiles through which diapause development may progress even though phenotypes may appear similar.

A key aspect of insect diapause is its anticipatory nature. Using various environmental cues, insects enter diapause prior to the start of unfavorable conditions. But many aspects of the environmental challenges diapausing insects face are totally unpredictable, including the severity, duration and frequency of individual stressors, as well as the temporal relationship between different environmental stressors. To survive the unpredictable complexity of environmental stressors, diapausing insects likely do not use a one-size-fits-all approach to overwintering. This plasticity has been demonstrated at the molecular level in a number of insect species. For example, in some diapausing insects, expression patterns of the heat shock proteins following a cold shock were determined by the insects' thermal histories [gypsy moth, *Lymantria dispar* (Lepidoptera: Erebidae), Yocom et al., 1991; Colorado potato beetle, *Leptinotarsa decemlineata*, Yocom, 2001]. Similarly, in the present study, we found differences in expression patterns between the four treatment groups at each time point surveyed. Together, these results suggest that there is a complex interaction between an insect's environmental history and current thermal conditions that regulate diapause development and which may vary between individuals even within the same geographic location.

The majority of our understanding of insects' molecular mechanisms for overwintering and diapause development has come from laboratory studies. Because of the differences in environmental conditions between the laboratory and field, laboratory studies may not yield a complete picture of the dynamic range of diapause physiology. Indeed, under laboratory conditions, gene expression patterns of non-stress-associated genes in Colorado potato beetle entering diapause appear to be consistent between individual beetles (Yocom et al., 2009a,b), yet in the field, beetles collected from the same area exhibited eight different expression patterns (Yocom et al., 2011). This disparity between laboratory and field results supports the hypothesis that there is more than one order of gene expression leading to diapause initiation. This conclusion was further supported by work done by Lehmann et al. (2014) showing population differences in gene expression profiles as Colorado potato beetles entered diapause. One reason for these discrepancies is that studies of gene expression during diapause development under laboratory conditions are normally conducted under constant temperatures. However, diapausing insects under field conditions are exposed to fluctuating temperatures. Rearing post-diapause quiescent *M. rotundata* prepupae under a fluctuating thermal regime significantly impacted gene expression patterns of wide categories of genes (Torson et al., 2015). Together, these studies strongly indicate that environmental history has a major impact on gene expression patterns during diapause development. Additionally, these studies suggest that it may be difficult to compare results from different investigations owing to differences in the environmental histories of the individuals being compared.

#### **Identifying a diapause 'toolkit'**

The hypothesis of a diapause 'genetic toolkit', which asserts that a conserved set of genes regulates diapause development across insect species, has been proposed by a number of research teams (Ragland et al., 2010; Poelchau et al., 2013a; Huestis and Lehmann, 2014; Amsalem et al., 2015; Yocom et al., 2015; Ragland and Keep, 2017). However, there is currently no agreement between the proposed lists of toolkit genes. The rationale for the existence of a toolkit is highly reasonable, given that there is only a limited number of regulatory pathways and checkpoints within those pathways for the regulation of diapause development. For example, it has been

well established that, depending on the developmental stage that enters diapause, either juvenile hormone or ecdysone is a part of the regulatory mechanism of diapause (Denlinger et al., 2005, 2011). The physiological effect of these hormones is exerted by regulating the rate of synthesis or degradation of the hormone, or by the differential regulation of the hormone receptor complex components. Therefore, at least with closely related insect species, the expectation for a common set of shared genes regulating diapause is based on solid physiological justification.

Nevertheless, a number of complexities compromise attempts to identify a diapause 'toolkit'. The first is that the insect's physiology is continuously changing as it proceeds through diapause development (Danks, 1987; Sawer et al., 1993; Koštál, 2006; Koštál et al., 2017, Yocom et al., 2006). At the transcriptional level, each phase (initiation, maintenance and termination) of diapause in the fly *Chymomyza costata* (Diptera: Drosophilidae) can be further subdivided into subphases with specific gene expression patterns with very little overlap in the differentially regulated genes between these different subphases (Koštál et al., 2017). The dynamic nature of diapause development can also be seen in how rapidly gene expression patterns can change. Exposing a diapausing apple maggot, *Rhagoletis pomonella* (Diptera: Tephritidae), to a permissive temperature for the resumption of direct development induced 1394 differentially regulated genes over the period examined. Of the genes differentially regulated between the 0 and 24 h time points, 75% had reversed their direction of expression by the 48 h time point (Meyers et al., 2016). Therefore, to identify a robust and reliable diapause toolkit, a method must first be established to insure that physiologically equivalent stages of diapause are being compared.

Another significant challenge facing the identification of a diapause toolkit is that insects experiencing diapause development under field conditions may be physiologically different from insects diapausing under laboratory conditions. In addition to those studies discussed above, adult firebugs, *Pyrrhocoris apterus* (Hemiptera: Pyrrhocoridae), whose diapause was terminated in the laboratory remained responsive to photoperiod, whereas those terminated under variable field conditions were nonresponsive to photoperiod (Hodek, 1968, 1983, in Koštál, 2006). Similarly, the median time for emergence from the overwintering substrate for postdiapausing Colorado potato beetle varied according to whether they were overwintered in the laboratory or the field (Tauber et al., 1988). Additionally, our study observed differences in gene expression between *M. rotundata* prepupae kept in the laboratory and the field. In light of all of these findings, a toolkit identified from experiments performed in controlled settings may not accurately reflect the physiological reality experienced by insects under natural environmental conditions. Development of an ecologically sound toolkit requires meeting the challenge of ensuring that physiologically equivalent stages are compared under relevant conditions. Therefore, developing a diapause toolkit of shared diapause-regulating genes may be technically challenging for all but a small group of closely related species with similar life histories.

The recently proposed hypothesis of omnigenics (Boyle et al., 2017) has major implications for the hypothesis of a genetic toolkit for complex traits such as diapause. The model of omnigenics proposes that complex traits (phenotypes) are directly impacted by a small number of genes that play an ascribed biological role in that trait as well as their direct regulators. These genes are referred to as core genes. But, owing to the interconnectivity of the regulatory pathways, any genes expressed are likely to affect the phenotype of a complex trait. A central tenet of omnigenics is that the core genes of

a complex trait are far outnumbered by these peripheral genes and that some complex traits may have no core genes at all. Classification of a particular gene as core or peripheral may be more a matter of degree than an either/or assignment. This ambiguity in classifying a gene as core or peripheral is yet another challenge in establishing a genetic toolkit for diapause.

The results presented here for *M. rotundata* suggest that the possible number of core genes (i.e. those genes shared between the four treatments in the between-month comparisons) may be as high as 406. A subset (130) of these potential core genes is shared between more than one comparison, increasing the likelihood that they are core genes (toolkit genes) (Table S3). Six of these genes are upregulated in four of the six possible between-month comparisons: November to March, November to May, January to March, and January to May. The physiological function of one of these six genes is currently unknown. The five remaining genes were compared with the list of differentially regulated genes isolated from *M. rotundata* diapausing and post-diapausing prepupae in Yocum et al. (2015). When directionality of expression is taken into consideration, only the gene *sex comb on midleg* (*Scm*) is shared between these two studies. The genes for both vitellogenin and phosphoglycolate phosphatase were downregulated whereas the gene for alkaline phosphate was not differentially regulated. One possible explanation for these discrepancies is that diapausing samples for Yocum et al. (2015) were collected in October rather than November as in this study.

The estimate of possible toolkit genes presented here is probably high, because the field samples used in this experiment may not be completely ecologically accurate for representing diapausing *M. rotundata*. One possible environmental factor not controlled for in this investigation was photoperiodism. The prepupae stored under laboratory conditions were kept in darkness and the field bees were exposed to the natural photoperiod. At the time of designing this experiment, *M. rotundata* was thought not to be sensitive to light (Tweedy and Stephen, 1970), a natural consequence of nesting in cavities. Under natural conditions, diapausing prepupae are cocooned and enclosed within a leaf-lined cell situated among a series of cells within a cavity. As such, light would be greatly restricted or totally blocked. We have recently discovered that developing *M. rotundata* are sensitive to light and that a limited amount of light can penetrate the leaf cell and cocoon (Bennett et al., 2018). If photoperiodism can account for a proportion of unexplained variance (75%) in the ANOVA model, this would strengthen our conclusion that the diapause transcriptome would vary between individuals based on their environmental history. In this hypothetical scenario, location and spatial orientation of the nest wherein some of the diapausing prepupae will be exposed to light and but not others will result in related gene expression differences. As more ecologically relevant experiments are developed, the number of possible core genes will likely decrease. Therefore, developing an accurate ecological understanding of diapause will require further understanding of the impact of peripheral genes upon a limited number of core genes.

## Conclusions

Environmental history influences gene expression patterns throughout the course of diapause development. The isolation of treatment-specific differentially regulated genes and the low level of overlap between these genes indicate that the prepupae were physiologically distinct at each time point examined. This study also underscores the need for future studies to establish that they are indeed comparing physiologically equivalent stages before

attempting to refine a genetic toolkit for diapause. Based on the results presented, we hypothesize that diapause is an omnigenic response and that the transcript expression profile of an individual insect is shaped more by its environmental history than by a single ‘toolkit’. The conserved signaling pathways and molecular processes observed in various dormancies across taxa (Hand et al., 2016) suggest that our hypothesis may have wider application beyond Insecta.

## Acknowledgements

The authors thank Marnie Larson of the USDA-ARS, Fargo, ND, USA, for her technical assistance. We thank Marnie Larson and Lisa Yocum for editing the various drafts of the manuscript submitted for publication. We thank Ellen Klomps, USDA-ARS, Logan, UT, USA, and Utah State University undergraduates Martin Welker and Amy Spielmaker for their extremely valuable assistance in nest collections and dissections plus data entry and coordination. We appreciate the very helpful critiques of two anonymous reviewers.

## Competing interests

The authors declare no competing or financial interests.

## Author contributions

Conceptualization: G.D.Y., T.L.P.; Software: A.K.C.; Formal analysis: A.K.C., A.R.; Resources: T.L.P.; Data curation: A.K.C.; Writing - original draft: G.D.Y.; Writing - review & editing: G.D.Y., A.K.C., J.P.R., A.R., T.L.P., K.J.G., J.H.B.; Supervision: G.D.Y., J.P.R.; Project administration: G.D.Y., J.P.R.

## Funding

This research was funded by the U.S. Department of Agriculture, Agricultural Research Service Project Plans 3060-21220-027-00D and 3060-21220-030-00D to G.D.Y. and J.P.R. Data were processed using cyberinfrastructure supported by the National Science Foundation under award numbers DBI-0735191 and DBI-1265383 (CyVerse, <http://www.cyverse.org/>).

## Data availability

Raw sequence data are deposited in NCBI's SRA database under SRA study SRP116229, BioProject PRJNA400265, as 16 BioSamples, one for each treatment group and collection date, with accessions SAMN07562395–SAMN07562410. Transcript assembly, along with its associated descriptions and GO term and KEGG pathway identifiers, is available through the i5k Workspace@NAL (<https://i5k.nal.usda.gov/megachile-rotundata>) and can be viewed in the genome browser (Poelchau et al., 2015).

## Supplementary information

Supplementary information available online at <http://jeb.biologists.org/lookup/doi/10.1242/jeb.173443.supplemental>

## References

- Aguissa-Touré, A.-H., Wong, R. P. and Li, G.** (2011). The ING family tumor suppressors: from structure to function. *Cell. Mol. Life Sci.* **68**, 45–54.
- Amsalem, E., Galbraith, D. A., Cnaani, J., Teal, P. E. A. and Grozinger, C. M.** (2015). Conservation and modification of genetic and physiological toolkit underpinning diapause in bumble bee queens. *Mol. Ecol.* **24**, 5596–5615.
- Belvin, M. P., Jin, Y. and Anderson, K. V.** (1995). Cactus protein degradation mediates *Drosophila* dorsal-ventral signaling. *Gene Dev.* **9**, 783–793.
- Benjamini, Y. and Hochberg, Y.** (1995). Controlling the false discovery rate: a practical and powerful approach to multiple testing. *J. R. Soc. Series B Methodol.* **57**, 289–300.
- Bennett, M. M., Rinehart, J. P., Yocum, G. D., Doekott, C. and Greenlee, K. J.** (2018). Cues for cavity nesters: investigating relevant zeitgebers for emerging leafcutting bees, *Megachile rotundata*. *J. Exp. Biol.* **221**, jeb175406.
- Boyle, E. A., Li, Y. I. and Pritchard, J. K.** (2017). An expanded view of complex traits: from polygenic to omnigenic. *Cell* **169**, 1177–1186.
- Camacho, C., Coulouris, G., Avagyan, V., Ma, N., Papadopoulos, J., Bealer, K. and Madden, T. L.** (2009). BLAST+: architecture and applications. *BMC Bioinformatics* **10**, 421.
- Campos, E. I., Chin, M. Y., Kuo, W. H. and Li, G.** (2004). Biological functions of the ING family tumor suppressors. *Cell. Mol. Life Sci.* **61**, 2597–2613.
- Cole, A. H. and Jones, S. N.** (2008). The ING gene family in the regulation of cell growth and tumorigenesis. *J. Cell Physiol.* **218**, 45–57.
- Conesa, A., Gotz, S., Garcia-Gomez, J. M., Terol, J. and Robles, M.** (2005). Blast2GO: a universal tool for annotation, visualization and analysis in functional genomics research. *Bioinformatics* **21**, 3674–3676.

- Cox, M. P., Peterson, D. A. and Biggs, P. J.** (2010). SolexaQA: At-a-glance quality assessment of Illumina second-generation sequencing data. *BMC Bioinformatics* **11**, 485.
- Danks, H. V.** (1987). *Insect Dormancy: An Ecological Perspective*. Ottawa, ON%: Biological Survey of Canada.
- Denlinger, D. L.** (2002). Regulation of diapause. *Annu. Rev. Entomol.* **47**, 93-122.
- Denlinger, D. L., Yocom, G. D. and Rinehart, J. P.** (2005). Hormonal control of diapause. In *Comprehensive Molecular Insect Science*, vol. 3 (ed. L. I. Gilbert, K. Iatrou and S. S. Gill), pp. 615-650. Oxford, UK: Elsevier.
- Denlinger, D. L., Yocom, G. D. and Rinehart, J. P.** (2011). Hormonal control of diapause. In *Insect Endocrinology* (ed. L. Gilbert), pp. 430-463. The Netherlands: Academic Press.
- Dong, Y., Desneux, N., Lei, C. and Niu, C.** (2014). Transcriptome characterization analysis of *Bactrocera minax* and new insight into its pupal diapause development with gene expression analysis. *Int. J. Biol. Sci.* **10**, 1051-1063.
- Doong, H., Vrailas, A. and Kohn, E. C.** (2002). What's in the 'BAG'?—a functional domain analysis of the BAG-family proteins. *Cancer Lett.* **188**, 25-32.
- Doyon, Y., Cayrou, C., Ullah, M., Landry, A.-J., Côté, V., Selleck, W., Lane, W. S., Tan, S., Yang, X.-J. and Côté, J.** (2006). ING tumor suppressor proteins are critical regulators of chromatin acetylation required for genome expression and perpetuation. *Mol. Cell* **21**, 51-60.
- Eisen, M. B., Spellman, P. T., Brown, P. O. and Botstein, D.** (1998). Cluster analysis and display of genome-wide expression patterns. *Proc. Natl. Acad. Sci. USA* **95**, 14863-14868.
- Emerson, K. J., Bradshaw, W. E. and Holzapfel, C. M.** (2010). Microarrays reveal early transcriptional events during the termination of larval diapause in natural populations of the mosquito, *Wyeomyia smithii*. *PLoS ONE* **5**, e9574.
- Enserink, J. M. and Kolodner, R. D.** (2010). An overview of CDK1-controlled targets and processes. *Cell Div.* **5**, 11.
- Gong, Z.-J., Wu, Y.-Q., Miao, J., Duan, Y., Jiang, Y.-L. and Li, T.** (2013). Global transcriptome analysis of orange wheat blossom midge, *Sitodiplosis mosellana* (Gehin) (Diptera: Cecidomyiidae) to identify candidate transcripts regulating diapause. *PLoS ONE* **8**, e71564.
- Hand, S. C., Denlinger, D. L., Podrabsky, J. E. and Roy, R.** (2016). Mechanisms of animal diapause: recent developments from nematodes, crustaceans, insects, and fish. *Am. J. Physiol. Regul. Integr. Comp. Physiol.* **310**, R1193-R1211.
- Hao, Y.-J., Zhang, Y.-J., Si, F.-L., Fu, D.-Y., He, Z.-B. and Chen, B.** (2016). Insight into the possible mechanism of the summer diapause of *Delia antiqua* (Diptera: Anthomyiidae) through digital gene expression analysis. *Insect Sci.* **23**, 438-451.
- Hobbs, G. A. and Richards, K. W.** (1976). Selection for a univoltine strain of *Megachile* (*Eutricharaea*) *pacifica* (Hymenoptera: Megachilidae). *Can. Entomol.* **108**, 165-167.
- Hodek, I.** (1968). Diapause in females of *Pyrrhocoris apterus* L. (Heteroptera). *Acta Entomol. Bohemoslov.* **65**, 422-435.
- Hodek, I.** (1983). Role of environmental factors and endogenous mechanisms in the seasonality of reproduction in insects diapausing as adults. In *Diapause and Life Cycle Strategies in Insects* (ed. V. K. Brown and I. Hodek), pp. 9-33. The Hague, The Netherlands: Dr. W. Junk Publishers.
- Huang, D. W., Sherman, B. T. and Lempicki, R. A.** (2009). Systematic and integrative analysis of large gene lists using DAVID bioinformatics resources. *Nat. Protoc.* **4**, 44-57.
- Huang, X., Poelchau, M. F. and Armbruster, P. A.** (2015). Global transcriptional dynamics of diapause induction in non-blood-fed and blood-fed *Aedes albopictus*. *PLoS Negl. Trop. Dis.* **9**, e0003724.
- Huestis, D. L. and Lehmann, T.** (2014). Ecophysiology of *Anopheles gambiae* s. l.: persistence in the Sahel. *Infect. Genet. Evol.* **28**, 648-661.
- Johansen, C. A. and Eves, J. D.** (1973). Effects of chilling, humidity and seasonal conditions on emergence of the alfalfa leafcutting bee. *Environ. Entomol.* **2**, 23-26.
- Joyce, D., Albanese, C., Steer, J., Fu, M., Bouzahzah, B. and Pestell, R. G.** (2001). NF- $\kappa$ B and cell-cycle regulation: the cyclin connection. *Cytokine Growth Factor. Rev.* **12**, 73-90.
- Kabbage, M. and Dickman, M. B.** (2008). The BAG proteins: a ubiquitous family of chaperone regulators. *Cell. Mol. Life Sci.* **65**, 1390-1402.
- Kanehisa, M. and Goto, S.** (2000). KEGG: kyoto encyclopedia of genes and genomes. *Nucleic Acids Res.* **28**, 27-30.
- Kang, D. S., Cotton, M. A., Denlinger, D. L. and Sim, C.** (2016). Comparative transcriptomics reveals key gene expression differences between diapausing and non-diapausing adults of *Culex pipiens*. *PLoS ONE* **11**, e0154892.
- Kapheim, K. M., Pan, H., Li, C., Salzberg, S. L., Puui, D., Magoc, T., Robertson, H. M., Hudson, M. E., Venkat, A., Fischman, B. J. et al.** (2015). Social evolution. Genomic signatures of evolutionary transitions from solitary to group living. *Science* **348**, 1139-1143.
- Kemp, W. P. and Bosch, J.** (2001). Postcocooning temperatures and diapause in the alfalfa pollinator *Megachile rotundata* (Hymenoptera: Megachilidae). *Ann. Entomol. Soc. Am.* **94**, 244-250.
- Kim, D., Pertea, G., Trapnell, C., Pimental, H., Kelley, R. and Saizberg, S. L.** (2013). TopHat2: accurate alignment of transcriptomes in the presence of insertions, deletions and gene fusions. *Genome Biol.* **14**, R36.
- Koštál, V.** (2006). Eco-physiological phases of insect diapause. *J. Insect Physiol.* **52**, 113-127.
- Koštál, V., Šimůnková, P., Kobelková, A. and Shimada, K.** (2009). Cell cycle arrest a hallmark of insect diapause: changes in gene transcription during diapause induction in the drosophilid fly (*Chymomyza costata*). *Insect Biochem. Mol. Biol.* **39**, 875-883.
- Koštál, V., Štětina, T., Poupartin, R., Korbelová, J. and Bruce, A. W.** (2017). Conceptual framework of the eco-physiological phases of insect diapause development justified by transcriptomic profiling. *Proc. Natl. Acad. Sci. USA* **114**, 8532-8537.
- Krunic, M. D.** (1972). Voltinism in *Megachile rotundata* (Hymenoptera: Megachilidae) in southern Canada. *Can. Entomol.* **104**, 185-188.
- Lehmann, P., Piironen, S., Kankare, M., Lytyinen, A., Paljakka, M. and Lindström, L.** (2014). Photoperiodic effect on diapause-associated gene expression trajectories in European *Leptinotarsa decemlineata* populations. *Insect Molecul. Biol.* **23**, 566-578.
- Maisonjeune, C., Guilleret, I., Vick, P., Weber, T., Andre, P., Beyer, T., Blum, M. and Constam, D. B.** (2009). Bicaudal C, a novel regulator of Dvl signaling abutting RNA-processing bodies, controls cilia orientation and leftward flow. *Development* **136**, 3019-3030.
- Malumbres, M. and Barbacid, M.** (2009). Cell cycle, CDKs and cancer: a changing paradigm. *Nat. Rev. Cancer* **9**, 153-166.
- Meyers, P. J., Powell, T. H. Q., Walden, K. O., Schieferrecke, A. J., Feder, J. L., Hahn, D. H., Robertson, H. M., Berlocher, S. H. and Ragland, G. J.** (2016). Divergence of the diapause transcriptome in apple maggot flies: winter regulation and post-winter transcriptional repression. *J. Exper. Biol.* **219**, 2613-2622.
- Moribe, Y., Niimi, T., Yamashita, O. and Yaginuma, T.** (2001). Samui, a novel cold-inducible gene, encoding a protein with a BAG domain similar to silencer of death domain (SODD/BAG-4), isolated from *Bombyx* diapause eggs. *Eur. J. Biochem.* **268**, 3432-3442.
- Moribe, Y., Shirota, T., Kamba, M., Niimi, T., Yamashita, O. and Yaginuma, T.** (2002). Differential expression of two cold-inducible genes, *Samui* and *sorbitol dehydrogenase*, in *Bombyx* diapause eggs exposed to low temperatures. *J. Insect Biotechnol. Sericol.* **71**, 167-171.
- Nabbi, A., McClurg, U. L., Thalappally, S., Almami, A., Mobaht, M., Bismar, T. A., Binda, O. and Riabowol, K. T.** (2017). ING3 promotes prostate cancer growth by activating the androgen receptor. *BMC Med.* **15**, 103.
- Nakagaki, M., Takei, R., Nagashima, E. and Yaginuma, T.** (1991). Cell cycles in embryos of the silkworm, *Bombyx mori*; G2-arrest at diapause stage. *Dev. Biol.* **200**, 223-229.
- Niehrs, C. and Acebron, S. P.** (2012). Mitotic and mitogenic Wnt signaling. *EMBO J.* **31**, 2705-2713.
- O'Neill, K. M., O'Neill, R. P., Kemp, W. P. and Delphia, C. M.** (2011). Effect of temperature on post-wintering development and total lipid content of alfalfa leafcutting bees. *Environ. Entomol.* **40**, 917-930.
- Park, S., Blaser, S., Marchal, M. A., Houston, D. W. and Sheets, M. D.** (2016). A gradient of maternal Bicaudal-C controls vertebrate embryogenesis via translational repression of mRNAs encoding cell fate regulators. *Development* **143**, 864-871.
- Peters, J.-M.** (2006). The anaphase promoting complex/cyclosome: a machine designed to destroy. *Nat. Rev. Mol. Cell Biol.* **7**, 644-655.
- Pitts-Singer, T. L. and Cane, J. H.** (2011). The alfalfa leafcutting bee, *Megachile rotundata*: the world's most intensively managed solitary bee. *Annu. Rev. Entomol.* **56**, 221-237.
- Poelchau, M. F., Reynolds, J. A., Denlinger, D. L., Elsik, C. G. and Armbruster, P. A.** (2011). A denovo transcriptome of the Asian tiger mosquito, *Aedes albopictus*, to identify candidate transcripts for diapause preparation. *BMC Genomics* **12**, 619.
- Poelchau, M. F., Reynolds, J. A., Elsik, C. G., Denlinger, D. L. and Armbruster, P. A.** (2013a). Deep sequencing reveals complex mechanisms of diapause preparation in the invasive mosquito, *Aedes albopictus*. *Proc. R. Soc. B.* **280**, 20130143.
- Poelchau, M. F., Reynolds, J. A., Elsik, C. G., Denlinger, D. L. and Armbruster, P. A.** (2013b). RNA-Seq reveals early distinctions and late convergence of gene expression between diapause and quiescence in the Asian tiger mosquito, *Aedes albopictus*. *J. Exper. Biol.* **216**, 4082-4090.
- Poelchau, M., Childers, C., Moore, G., Tsavatapalli, V., Evans, J., Lee, C.-Y., Lin, J.-W. and Hackett, K.** (2015). The i5k Workspace@ NAL—enabling genomic data access, visualization and curation of arthropod genomes. *Nucleic Acids Res.* **43**, D714-D719.
- Qi, X., Zhang, L., Han, Y., Ren, X., Huang, J. and Chen, H.** (2015). De novo transcriptome sequencing and analysis of *Coccinella septempunctata* L. in non-diapause, diapause and diapause-terminated states to identify diapause-associated genes. *BMC Genomics* **16**, 1086.
- Ragland, G. J. and Keep, E.** (2017). Comparative transcriptomics support evolutionary convergence of diapause responses across Insecta. *Physiol. Entomol.* **42**, 246-256.
- Ragland, G. J., Denlinger, D. L. and Hahn, D. A.** (2010). Mechanisms of suspended animation are revealed by transcript profiling of diapause in the flesh fly. *Proc. Natl. Acad. Sci. USA* **107**, 14909-14914.
- Ragland, G. J., Egan, S. P., Feder, J. L., Berlocher, S. H. and Hahn, D. A.** (2011). Developmental trajectories of gene expression reveal candidates for diapause termination: a key life-history transition in the apple maggot fly *Rhagoletis pomonella*. *J. Exper. Biol.* **214**, 3948-3960.

- Ray, P., Zhang, D.-H., Elias, J. A. and Ray, A.** (1995). Cloning of a differentially expressed I $\kappa$ B-related protein. *J Biol. Chem.* **270**, 10680-10685.
- Sawer, A. J., Tauber, M. J., Tauber, C. A. and Ruberson, J. R.** (1993). Gypsy moth (Lepidoptera: Lymantriidae) egg development; a simulation analysis of laboratory and field data. *Ecol. Modelling* **66**, 121-155.
- Simão, F. A., Waterhouse, R. M., Ioannidis, P., Kriventseva, E. V. and Zdobnov, E. M.** (2015). BUSCO: assessing genome assembly and annotation completeness with single-copy orthologs. *Bioinformatics* **31**, 3210-3212.
- Tammaro, S. P. and Denlinger, D. L.** (1998). G0/G1 cell arrest in the brain of *Sarcophaga crassipalpis* during pupal diapause and the expression of the cell cycle regulator, proliferating cell nuclear antigen. *Insect Biochem. Mol. Biol.* **28**, 83-89.
- Tauber, M. J., Tauber, C. A. and Masaki, S.** (1986). *Seasonal Adaptations in Insects*. Oxford, UK: Oxford University Press.
- Tauber, M. J., Tauber, C. A., Obrycki, J. J., Gollands, B. and Wright, R. J.** (1988). Geographical variation in responses to photoperiod and temperature by *Leptinotarsa decemlineata* (Coleoptera: Chrysomelidae) during and after diapause. *Ann. Entomol. Soc. Am.* **81**, 764-773.
- Torson, A., Yocom, G. D., Rinehart, J. P., Kemp, W. P. and Bowsher, J. H.** (2015). Transcriptional responses to fluctuating thermal regimes underpinning differences in survival in the solitary bee *Megachile rotundata*. *J. Exper. Biol.* **218**, 1060-1068.
- Trapnell, C., Roberts, A., Goff, L., Pertea, G., Kim, D., Kelly, D. R., Pimental, H., Saizber, S. L., Rinn, J. L. and Pachter, L.** (2012). Differential gene and transcript expression analysis of RNA-seq experiments with TopHat and Cufflinks. *Nat. Protoc.* **7**, 562-578.
- Tweedy, D. G. and Stephen, W. P.** (1970). Light refractive emergence rhythm in the leafcutter bee, *Megachile rotundata* (F.) (Hymenoptera: Apoidea). *Experientia* **26**, 377-379.
- Yocom, G. D.** (2001). Differential expression of two *HSP70* transcripts in response to cold shock, thermoperiod, and adult diapause in the Colorado potato beetle. *J. Insect Physiol.* **47**, 1139-1145.
- Yocom, G. D., Joplin, K. H. and Denlinger, D. L.** (1991). Expression of heat shock proteins in response to high and low temperature extremes in diapausing pharate larvae of the gypsy moth, *Lymantria dispar*. *Arch. Insect Biochem. Physiol.* **18**, 239-249.
- Yocom, G. D., Kemp, W. P., Bosch, J. and Knoblett, J. N.** (2006). Thermal history influences diapause development in the solitary bee *Megachile rotundata*. *J. Insect Physiol.* **52**, 1113-1120.
- Yocom, G. D., Rinehart, J. P. and Larson, M. L.** (2009a). Down-regulation of gene expression between the diapause initiation and maintenance phases of the Colorado potato beetle, *Leptinotarsa decemlineata* (Coleoptera: Chrysomelidae). *Eur. J. Entomol.* **106**, 471-476.
- Yocom, G. D., Rinehart, J. P., Chirumamilla-Chapara, A. and Larson, M. L.** (2009b). Characterization of gene expression patterns during the initiation and maintenance phases of diapause in the Colorado potato beetle, *Leptinotarsa decemlineata*. *J. Insect Physiol.* **22**, 32-39.
- Yocom, G. D., Rinehart, J. P. and Larson, M. L.** (2011). Monitoring diapause development in the Colorado potato beetle, *Leptinotarsa decemlineata*, under field conditions using molecular biomarkers. *J. Insect Physiol.* **57**, 645-652.
- Yocom, G. D., Rinehart, J. P., Horvath, D. P., Kemp, W. P., Bosch, J., Alroobi, R. and Salem, S.** (2015). Key molecular processes of the diapause to post-diapause quiescence transition in the alfalfa leafcutting bee *Megachile rotundata* identified by comparative transcriptome analysis. *Physio. Entomol.* **40**, 103-112.
- Young, M. D., Wakefield, M. J., Smyth, G. K. and Oshlack, A.** (2010). Gene ontology analysis for RNA-seq: accounting for selection bias. *Genome Biol.* **11**, R14.

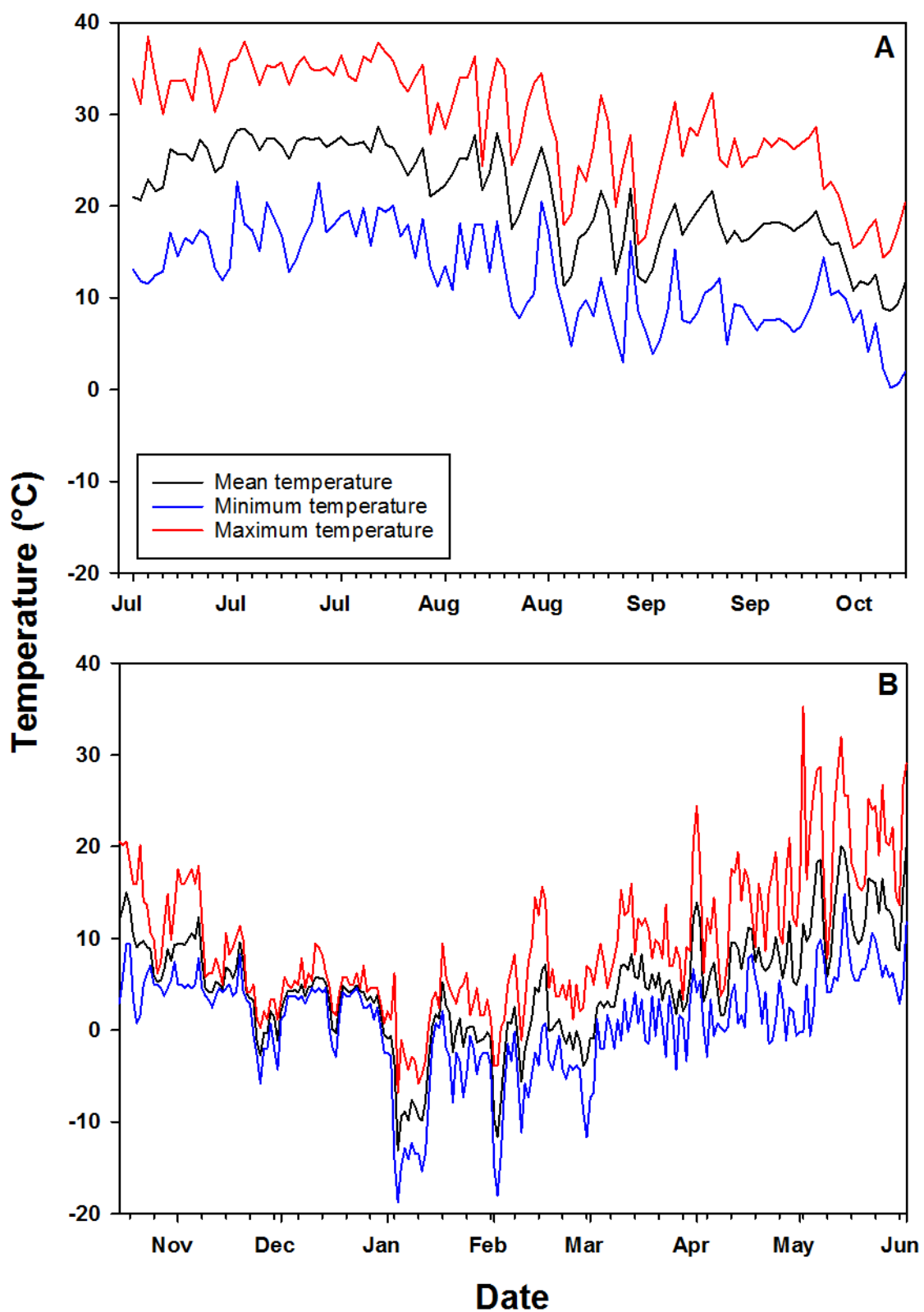


Figure S1. Temperature plots for the open shelter (A) Summer temperatures experienced by all developing larvae before 22 October, 2010 and (B) temperatures experienced by the diapausing prepupae that remained outdoors after October 22, 2010.

Table S1. Raw, paired-end RNA-seq reads from each biological replicate were mapped to the *M. rotundata* genome

SampleID <sup>1</sup>	# Reads						% Discarded for Quality	TopHat2 Alignment Summary (Reads After Quality Trimming)										
	Left Reads			Right Reads				Unpaired Reads		Overall read mapping rate	Aligned pairs	Concordant pair alignment rate						
	Lane 7 R1	Lane 7 R2	Lane 8 R1	Lane 8 R2	Total Left Reads	Total Right Reads		Input	Mapped			Input	Mapped					
ENovLabA	4009364	4009364	4014503	4014503	8023867	8023867	13.0%	6573224	5910369	6573224	5961452	809837	745780	90.4%	5768220	87.6%		
ENovLabB	4639029	4639029	4633618	4633618	9272647	9272647	13.0%	7595698	6615317	7595698	6697386	935233	836899	87.7%	6433865	84.6%		
ENovLabC	3946336	3946336	3939500	3939500	7885836	7885836	13.1%	6445919	5639350	6445919	5720239	809802	720609	88.2%	5474655	84.7%		
LNovLabA	4226056	4226056	4224573	4224573	8450629	8450629	14.0%	6794171	6011645	6794171	6086162	938455	852307	89.1%	5834531	85.7%		
LNovLabB	6218415	6218415	6226477	6226477	12444892	12444892	14.7%	9913011	8475092	9913011	8612225	1414333	1254084	86.4%	8213409	82.8%		
LNovLabC	4783233	4783233	4785685	4785685	9568918	9568918	14.1%	7700263	6854841	7700263	6931758	1046099	951200	89.6%	6661652	86.4%		
LNovFieldA	5508410	5508410	5521375	5521375	11029785	11029785	13.9%	8893729	7664568	8893729	7753770	1216493	1081213	86.8%	7438494	83.5%		
LNovFieldB	4531090	4531090	4551964	4551964	9083054	9083054	14.2%	7295783	6694770	7295783	6754121	995087	927171	92.2%	6522506	89.1%		
LNovFieldC	4125909	4125909	4131265	4131265	8257174	8257174	13.4%	6721060	5890591	6721060	5949428	855249	774746	88.2%	5726379	85.1%		
EJanLabA	5005756	5005756	5004639	5004639	10010395	10010395	14.2%	8034312	6754768	8034312	6870531	1103770	960979	84.9%	6551359	81.4%		
EJanLabB	4369536	4369536	4367284	4367284	8736820	8736820	14.1%	7032025	5994495	7032025	6088317	954132	831260	86.0%	5807093	82.4%		
EJanLabC	4214005	4214005	4209459	4209459	8423464	8423464	14.1%	6774720	5809951	6774720	5900224	924018	810203	86.5%	5628990	82.9%		
ENovFieldA	4670065	4670065	4683671	4683671	9353736	9353736	14.2%	7501039	6326922	7501039	6429146	1040147	905512	85.2%	6120223	81.4%		
ENovFieldB	4397626	4397626	4387100	4387100	8784726	8784726	13.9%	7098050	6179086	7098050	6262796	930433	832507	87.8%	6007881	84.6%		
ENovFieldC	3895903	3895903	3893475	3893475	7789378	7789378	13.5%	6334793	5611037	6334793	5679930	813606	734690	89.2%	5456176	86.0%		
LJanLabA	3971640	3971640	3966644	3966644	7938284	7938284	13.7%	6425936	5690885	6425936	5766986	850798	768854	89.2%	5525167	85.8%		
LJanLabB	3191935	3191935	3194069	3194069	6386004	6386004	14.0%	5133248	4599343	5133248	4657198	714040	649780	90.2%	4468874	86.9%		
LJanLabC	4365157	4365157	4368025	4368025	8733182	8733182	15.6%	6815567	6058640	6815567	6129611	1109488	1019022	89.6%	5900147	84.3%		
EJanFieldA	5760248	5760248	5777850	5777850	11538098	11538098	13.5%	9371762	7805913	9371762	7932073	1226198	1060002	84.1%	7556576	80.5%		
EJanFieldB	4067961	4067961	4087156	4087156	8155117	8155117	13.8%	6585755	5957567	6585755	6003732	893876	825671	90.9%	5807943	87.9%		
EJanFieldC	4184762	4184762	4190204	4190204	8374966	8374966	13.6%	6792478	5777522	6792478	5868950	895128	785652	85.9%	5604596	82.3%		
LJanFieldA	4629197	4629197	4637957	4637957	9267154	9267154	15.0%	7312895	6523103	7312895	6598841	1127387	1037261	89.9%	6351361	85.2%		
LJanFieldB	4251354	4251354	4257266	4257266	8508620	8508620	13.1%	6955853	6134724	6955853	6204373	878096	791801	88.8%	5953462	85.3%		
LJanFieldC	5148636	5148636	5152766	5152766	10301402	10301402	13.2%	8408984	7491364	8408984	7560976	1068227	971522	89.6%	7275749	86.4%		
EMarFieldA	3374960	3374960	3371592	3371592	6746552	6746552	11.4%	5669396	5105748	5669396	5150997	614302	561092	90.5%	4976356	87.6%		
EMarFieldB	3875524	3875524	3871607	3871607	7747131	7747131	13.1%	6331075	5508978	6331075	5581371	800666	712463	87.7%	5348251	84.3%		
EMarFieldC	3808968	3808968	3811521	3811521	7620489	7620489	13.6%	6182926	5384619	6182926	5454320	806591	721950	87.8%	5233902	84.5%		
LMarFieldA	4108414	4108414	4101106	4101106	8209520	8209520	13.7%	6639340	5817599	6639340	5895863	887369	795161	88.3%	5647294	84.9%		
LMarFieldB	4599980	4599980	4616577	4616577	9216557	9216557	13.6%	7476209	6633961	7476209	6715706	981791	889587	89.4%	6448510	86.1%		
LMarFieldC	4306285	4306285	4323726	4323726	8630011	8630011	13.7%	6979075	6201360	6979075	6271255	934714	841451	89.4%	6025512	86.1%		
EMarLabA	4139509	4139509	4147196	4147196	8286705	8286705	13.3%	6755541	6000199	6755541	6073354	863968	779951	89.4%	5826757	86.1%		
EMarLabB	4271852	4271852	4266610	4266610	8538462	8538462	13.4%	6939157	6095431	6939157	6183208	910938	808987	88.5%	5912110	85.0%		
EMarLabC	3824114	3824114	3817714	3817714	7641828	7641828	13.7%	6186280	5374546	6186280	5454882	821158	724328	87.6%	5207946	84.0%		
LabArLabA	3760553	3760553	3754015	3754015	7514568	7514568	14.0%	6049166	5188647	6049166	5265970	828942	725540	86.5%	5027424	82.8%		
LabArLabB	4084011</td																	

Table S2. Differentially regulated genes for the within-month, between-month comparisons and November field versus laboratory comparisons.

Differentially regulated genes common to all within month treatment comparisons.

November Down Regulated Genes		Fold change				
Gene_ID	Description	ELab versus LLab	ELab versus EField	EField versus LField	LLab versus LField	
XLOC_002189	transcription factor SOX-11	-0.941127	-0.669238	-1.155	-0.883115	
XLOC_003692	xxa-Pro aminopeptidase 1-like	-1.7173	-2.21259	-1.51848	-2.01377	
XLOC_005534	putative fatty acyl-CoA reductase CG5065-	-1.04456	-0.640885	-1.34868	-0.945006	
XLOC_006049	tyrosine hydroxylase isoform X1	-1.43081	-2.0184	-1.37369	-1.96129	
XLOC_008673	NA	-1.53605	-2.44247	-2.88614	-3.79257	
XLOC_011899	elongation of very long chain fatty acids	-1.65802	-1.77167	-0.744568	-0.858215	
November Up Regulated Genes		Fold change				
Gene_ID	Description	ELab versus LLab	ELab versus EField	EField versus LField	LLab versus LField	
XLOC_004761	hexamerin 70b precursor	2.34809	1.46161	2.5034	1.61692	
XLOC_009125	lipase 1-like isoform X1; lipase 1-like	1.29764	1.14252	1.41126	1.25614	
XLOC_011394	leucine-rich repeat neuronal protein 1-like	0.860734	1.212	0.722264	1.07353	
January Down Regulated Genes		Fold change				
Gene_ID	Description	ELab versus LLab	ELab versus EField	EField versus LField	LLab versus LField	
XLOC_001549	SCO-spondin	-0.725805	-0.892716	-1.07614	-1.24305	
XLOC_001887	mannan-binding lectin serine protease 1	-1.8118	-1.58881	-1.70699	-1.48399	
XLOC_003416	aminopeptidase N-like isoform X2	-1.00299	-1.11276	-0.637316	-0.747086	
XLOC_004315	cuticular protein analogous to peritrophins	-0.808169	-0.925752	-1.98758	-2.10516	
XLOC_010014	3-C precursor; cuticular protein analogous LOW QUALITY PROTEIN: ceramide	-1.0754	-0.864981	-0.934659	-0.724239	
XLOC_010272	3-C precursor; cuticular protein analogous to peritrophins	-0.865913	-0.814446	-1.4738	-1.42233	
XLOC_010554	probable G-protein coupled receptor No9-	-0.706402	-0.690315	-0.82978	-0.813693	
XLOC_011899	elongation of very long chain fatty acids	-1.36377	-1.27009	-2.13523	-2.04155	
XLOC_012808	DNA-directed RNA polymerase II subunit	-0.0074	-0.965636	-1.05868	-1.01692	
XLOC_013034	RPB1-like isoform X1	-0.804889	-0.947197	-1.08786	-1.23016	
XLOC_013484		uncharacterized threonine-rich GPI-anchored glycoprotein PJ4664.02 isoform X2; uncharacterized threonine-rich GPI-anchored glycoprotein PJ4664.02 isoform X3; uncharacterized threonine-rich GPI-anchored glycoprotein PJ4664.02 isoform X4; uncharacterized threonine-rich GPI-anchored glycoprotein PJ4664.02 isoform X1	-0.670477	-0.769301	-0.624879	-0.723704
January Up Regulated Genes		Fold change				
Gene_ID	Description	ELab versus LLab	ELab versus EField	EField versus LField	LLab versus LField	
XLOC_002659	60S ribosomal protein L12 isoform X1; protein crooked neck	1.3007	1.09909	1.20549	1.00387	
XLOC_003131	NA	1.10362	0.980299	1.60793	1.4846	
XLOC_003387	60S ribosomal protein L10a; regulator of telomere elongation helicase 1 homolog	1.33562	1.06454	1.44004	1.16896	
XLOC_004761	hexamerin 70b precursor	1.09861	1.00172	2.05454	1.95765	
XLOC_005056	glutathione S-transferase D1 isoform X5	0.602881	0.644806	0.732305	0.774229	
XLOC_006692	cytochrome P450 6A5S; cytochrome P450 6a2-like	2.36321	1.47168	3.10944	2.21792	
XLOC_007083	glutathione S-transferase S1 isoform X1	0.909572	0.895485	0.969188	0.955101	
XLOC_008483	solute carrier family 28 member 3-like; solute carrier family 28 member 3-like isoform X1; Protein lozenge; NA	1.41558	1.27714	2.91717	2.77874	
XLOC_009125	lipase 1-like isoform X1; lipase 1-like isoform X3; lipase 1-like isoform X4	0.927597	0.937431	0.795193	0.805026	
XLOC_012798	peroxisomal hydratase-dehydrogenase-epimerase-like	1.71794	1.16415	1.54506	0.991266	
March Down Regulated Genes		Fold change				
Gene_ID	Description	ELab versus LLab	ELab versus EField	EField versus LField	LLab versus LField	
XLOC_001549	SCO-spondin	-0.965646	-0.660959	-1.13057	-0.825879	
XLOC_003960	spermosin-like	-1.08147	-0.835407	-1.39142	-1.14536	
XLOC_004315	cuticular protein analogous to peritrophins	-1.59555	-0.747776	-1.97156	-1.12379	
XLOC_005430	3-C precursor; cuticular protein analogous to peritrophins	-3.49378	-2.76516	-2.90452	-2.1759	
XLOC_006052	chemosensory protein 6 precursor	-1.07229	-0.985236	-1.02953	-0.942477	

XLOC_006089	Aggrecan core protein; macrophage mannose receptor 1-like; Macrophage mannose receptor 1	-1.6674	-1.7056	-1.47392	-1.51212
XLOC_012381	NA	-3.34337	-2.52899	-2.52318	-1.7088
XLOC_012808	DNA-directed RNA polymerase II subunit RPB1-like isoform X1	-1.06259	-0.745797	-1.06818	-0.751392
XLOC_013034	circadian clock-controlled protein-like	-0.660955	-0.736452	-1.44168	-1.51717

March Up Regulated Genes		Fold change			
Gene_ID	Description	E Lab versus L Lab	E Lab versus E Field	E Field versus L Field	L Lab versus L Field
XLOC_011375	NA	1.30667	1.40217	2.0821	2.17761

May Down Regulated Genes		Fold change			
Gene_ID	Description	E Lab versus L Lab	E Lab versus E Field	E Field versus L Field	L Lab versus L Field
XLOC_002473	beta-galactosidase-like isoform X1	-1.11508	-1.64051	-1.07592	-1.60135
XLOC_004641	glutamine synthetase	-0.867231	-1.85446	-1.2835	-2.27073
XLOC_005072	protein henna-like isoformX2; protein	-0.900039	-0.989448	-0.850091	-0.939501
XLOC_007963	henna-like isoform X3	-1.75146	-5.34541	-0.79053	-4.38448
XLOC_011896	endochitinase isoform 2	-3.32288	-2.87478	-3.0701	-2.622
elongation of very long chain fatty acids					
protein AAEL008004-like					

May Up Regulated Genes		Fold change			
Gene_ID	Description	E Lab versus L Lab	E Lab versus E Field	E Field versus L Field	L Lab versus L Field
XLOC_003421	GATA zinc finger domain-containing protein 4-like; uncharacterized protein LOC100874762; uncharacterized protein LOC100877006; NA	2.02065	2.92577	2.81938	3.72451

Differentially regulated genes common to all between month treatment comparisons.

November versus January Down Regulated Genes		Fold change			
Gene_ID	Description	E Lab	L Lab	E Field	L Field
XLOC_000319	NA	-5.57203	-5.38854	-4.27024	-2.46522
XLOC_000338	UNKNOWN	-2.20899	-6.54221	-3.15004	-2.53936
XLOC_000445	NA	-2.58754	-3.48641	-1.89729	-2.14823
XLOC_000492	unknown protein	-2.19801	-5.99257	-3.36955	-3.58422
XLOC_000521	uncharacterized protein LOC100865969	-2.36156	-6.24828	-3.01325	-2.83573
XLOC_000638	NA	-5.23218	-5.25043	-3.90021	-2.30674
XLOC_000639	NA	-4.45344	-5.62228	-3.77735	-2.54694
XLOC_000640	UNKNOWN	-2.47775	-5.42771	-2.5441	-3.09705
XLOC_000662	senescence-associated protein, putative circadian locomoter output cycles protein	-2.27484	-6.61065	-2.90356	-2.97127
XLOC_000671	kaput	-1.28461	-1.53328	-1.30469	-1.48495
XLOC_000826	RRNA intron-encoded homing endonuclease	-1.96953	-6.01487	-2.98188	-3.40341
XLOC_000868	NA	-4.78754	-5.58173	-3.65091	-2.30472
XLOC_001092	AAEL006178-PA	-0.762394	-0.753228	-1.23459	-0.67708
XLOC_001195	Protein Bm117	-2.10654	-6.39407	-2.619	-2.97503
XLOC_001360	inactive tyrosine-protein kinase 7-like	-1.37323	-1.56781	-1.2229	-1.76103
XLOC_001561	nuclear factor of activated T-cells 5; NA	-1.54954	-1.89593	-0.703516	-1.15714
XLOC_001688	ataxin-2 homolog isoform X1	-2.93379	-2.64762	-1.15642	-1.6005
XLOC_001702	senescence-associated protein, putative zinc finger and SCAN domain-containing	-2.25073	-6.47916	-3.00822	-3.01393
XLOC_001767	protein 22-like	-1.64251	-1.79439	-0.895671	-1.19529
XLOC_002075	X-box-binding protein	-1.77115	-2.12681	-0.846459	-0.94136
XLOC_002082	putative epidermal cell surface receptor-like isoform X3; putative epidermal cell surface receptor-like isoform X4; putative epidermal cell surface receptor-like isoform X1	-1.01376	-0.937569	-1.08344	-1.79722
XLOC_002189	transcription factor SOX-11	-2.20157	-1.86444	-1.34079	-1.28633
XLOC_002516	uncharacterized protein LOC100883637; protein kibra-like isoformX1; protein kibra-like isoform X3; hemK methyltransferase family member 1-like; protein kibra-like isoformX2	-1.4331	-1.37388	-1.20705	-1.02245
XLOC_002916	alpha-L1 nicotinic acetyl choline receptor	-2.29252	-6.48402	-3.02798	-3.19428
XLOC_003370	Ac1147-like protein	-2.19278	-6.20742	-2.60571	-4.28867
XLOC_003416	aminopeptidase N-like isoform X2	-0.978142	-0.736696	-0.881185	-1.79864

XLOC_003465	rho GTPase-activating protein 7 isoform				
XLOC_003466	X1; rho GTPase-activating protein 7				
	isoform X2	-1.68253	-1.54542	-0.89979	-1.16385
	NA	-1.44183	-1.09236	-0.900408	-1.19739
XLOC_003523	kynurenine/alpha-amino adipate				
XLOC_003656	aminotransferase, mitochondrial-like	-1.55482	-4.75423	-1.37414	-3.4328
XLOC_003692	NA	-6.62671	-6.22723	-5.15329	-1.47904
	xaa-Pro aminopeptidase 1-like	-5.02596	-4.2753	-3.18323	-2.49716
XLOC_003804	oxidative stress-induced growth inhibitor 1-like isoform X3; oxidative stress-induced				
XLOC_003966	growth inhibitor 1-like isoform X1	-0.846571	-0.68657	-0.867905	-0.77487
	HIG1 domain family member 1B-like	-2.28272	-2.47267	-0.639707	-1.01319
XLOC_004156	unknown; uncharacterized protein				
	LOC102670919 isoform X1;				
	uncharacterized protein LOC100884121; PWWP domain-containing protein 2B	-0.84222	-1.26431	-0.917575	-0.76205
XLOC_004486	uncharacterized protein LOC100865969	-2.59095	-6.36885	-3.11873	-2.83566
XLOC_004530	NA	-5.16397	-4.19106	-2.03456	-1.00247
XLOC_004603	homeobox protein caupolicana isoform X4; homeobox protein caupolicana isoform X3; NA	-1.73038	-1.49206	-1.13892	-0.71084
XLOC_005010	rootletin-like isoform X2; rootletin-like	-1.28021	-2.37767	-1.27213	-1.64126
XLOC_005067	isoform X3	-2.33386	-5.9343	-2.66373	-3.99007
XLOC_005103	Ac1147 dehydrogenase/reductase SDR family				
XLOC_006055	member 11-like isoform X1	-1.01022	-1.75248	-0.784897	-1.30746
XLOC_006709	heat shock protein 90	-2.47416	-2.78036	-0.721791	-0.78304
XLOC_006720	hypothetical protein V426_1069	-3.83486	-2.62762	-2.61358	-2.5276
XLOC_006721	protein TIS11-like; NA	-1.87102	-1.92597	-0.925934	-1.28104
XLOC_006905	protein TIS11-like	-3.97308	-4.15565	-0.877181	-1.66512
	protein split ends-like	-1.89119	-2.12288	-0.661831	-1.02337
XLOC_006935	ATP-binding cassette sub-family A member 2-like isoform X2; tubulin polyglutamylase complex subunit 2-like	-2.80768	-2.38724	-1.30988	-1.44863
	periaxin-like; zinc finger protein 704-like				
	isoform X3; zinc finger protein 704-like				
	isoform X2; flocculation protein FLO11				
XLOC_007013	isoform X3	-1.43951	-2.45303	-0.982273	-1.12307
XLOC_007473	AT-rich interactive domain-containing protein 5B-like isoform X2	-2.32192	-2.41108	-1.073	-0.73537
XLOC_007474	LIM domain-binding protein 2-like isoform X5; LIM domain-binding protein 2-like isoform X4; LIM domain-binding protein 2-like isoform X1; LIM domain-binding protein 2-like isoform X6; LIM domain-binding protein 2-like isoform X2	-1.75173	-1.43464	-0.85454	-0.76001
XLOC_007654	serine/arginine repetitive matrix protein 1	-1.17381	-1.51717	-1.32391	-2.07895
XLOC_007660	serine protease nudel	-1.58997	-0.718967	-0.672725	-0.77314
XLOC_008108	serine protease 53; carboxypeptidase B-like	-4.44997	-5.04977	-3.5466	-4.09326
XLOC_008483	solute carrier family 28 member 3-like; solute carrier family 28 member 3-like				
XLOC_008673	isoform X1; Protein lozenge; NA	-6.58907	-4.39825	-4.16446	-1.521
	NA	-5.7603	-5.4357	-3.96923	-2.18731
XLOC_008736	uncharacterized protein LOC100882035	-1.53366	-1.56295	-1.21293	-1.02127
XLOC_008947	adenomatous polyposis coli protein-like	-2.20613	-2.17733	-0.954543	-1.03607
XLOC_009164	cell wall protein AWA1-like isoform X2; zinc finger protein 182-like; NA	-1.63054	-1.58256	-1.78794	-1.17052
XLOC_009265	tRNA 2-thiocytidine biosynthesis protein TtcA	-0.764956	-0.808424	-0.981738	-0.7954
XLOC_009306	actin cytoskeleton-regulatory complex protein PAN1-like; NA	-5.01461	-3.24985	-2.24969	-2.137
XLOC_009453	rab11 family-interacting protein 4-like isoform X3; rab11 family-interacting protein 4-like isoform X2; rab11 family-interacting protein 4-like isoform X1; NA	-1.25537	-1.19828	-0.83747	-0.60497
XLOC_009805	ets DNA-binding protein pokkuri-like isoform X1	-2.22152	-2.11953	-0.946229	-1.87299
XLOC_010075	AP2-associated protein kinase 1-like isoform X3; NA; AP2-associated protein kinase 1-like isoform X1	-0.829878	-0.720419	-0.798596	-0.69176
XLOC_010166	NA	-2.19015	-5.97248	-2.71033	-4.00479

XLOC_010474	SH3 and multiple ankyrin repeat domains protein 3-like	-1.32074	-1.25999	-0.677563	-1.05695
XLOC_010852	protein TAR1-like	-2.21607	-6.25162	-3.00114	-2.97265
XLOC_010853	uncharacterized protein LOC101742759 activator of 90 kDa heat shock protein	-2.1535	-6.32285	-3.04875	-3.11465
XLOC_011050	ATPase homolog 1-like isoform 2	-1.57647	-1.81303	-1.06953	-0.7017
XLOC_011166	Zinc finger protein 40; NA	-2.31089	-2.88786	-1.4589	-0.93006
XLOC_011490	cadherin-23-like	-1.78362	-1.37342	-1.58583	-2.34799
XLOC_011519	flavin-containing monooxygenase FMO GS-OX-like 4-like	-1.46569	-3.83546	-1.86889	-1.78182
XLOC_011887	general transcriptional corepressor trfA-like	-1.06098	-0.572566	-0.637688	-0.72029
XLOC_012572	whirlin-like isoform X6; whirlin-like isoform X5; whirlin-like isoform X7	-2.80454	-2.68004	-2.22694	-1.25347
XLOC_012582	brain-specific angiogenesis inhibitor 1-like isoform X2	-2.84038	-2.79411	-1.40833	-1.45682
XLOC_012609	ecdysteroid-regulated gene E74 isoform X9; ecdysteroid-regulated gene E74 isoform X10	-1.08314	-0.726161	-1.20413	-1.5187
XLOC_012682	autophagy protein 5	-4.48768	-4.03295	-2.40404	-1.68418
XLOC_012974	histone-lysine N-methyltransferase 2C zinc finger SWIM domain-containing protein 8-like isoform X1; zinc finger SWIM domain-containing protein 8-like isoform X3	-5.09554	-4.50474	-1.34377	-1.44417
XLOC_013237	hypothetical protein EAG_08451; Protein CBG18438	-0.856287	-0.700345	-0.864834	-0.84995
XLOC_013272	TOX high mobility group box family member 3-like isoform X3; TOX high mobility group box family member 3-like isoform X1; TOX high mobility group box family member 3-like isoform X2	-1.12219	-1.16801	-0.707151	-1.0116
XLOC_013450		-1.73656	-1.33086	-0.658507	-0.77184

## November versus January Up Regulated Genes

Gene_ID	Description	Fold change			
		ELab	LLab	EField	LField
XLOC_002720	E3 ubiquitin-protein ligase RNF13-like isoform X3	0.759907	1.06183	0.788746	1.13943
XLOC_003688	DNA-dependent protein kinase catalytic subunit-like	1.52998	1.29414	0.990234	0.881082
XLOC_004384	NA	2.31095	1.01827	2.02181	1.31126
XLOC_008632	probable cation-transporting ATPase 13A3-like isoform X3; probable cation-transporting ATPase 13A3-like isoform X1	1.4763	1.56833	1.70405	1.29341
XLOC_010089	retrovirus-related Pol polyprotein from transposon 412	0.805516	1.14459	0.824858	0.825232
XLOC_010888	protein AF-10-like isoform X1	0.904179	0.979349	0.946853	0.831786
XLOC_011978	slit homolog 2 protein-like	1.27729	1.58574	0.943433	0.815088
XLOC_013342	CRE-binding bZIP protein SKO1-like	2.0029	1.72674	1.51192	1.59286

## November versus March Down Regulated Genes

Gene_ID	Description	Fold change			
		ELab	LLab	EField	LField
XLOC_000319	NA	-6.39625	-5.91341	-3.71982	-1.93443
XLOC_000445	NA	-3.09503	-3.67297	-2.18319	-2.37024
XLOC_000567	Bone morphogenetic protein 3; Bone morphogenetic protein glutamate receptor, ionotropic kainate 2-like	-1.40359	-0.761931	-1.31276	-0.97403
XLOC_000592	NA	-6.0028	-4.76087	-3.57571	-3.13661
XLOC_000638	NA	-6.11556	-5.8062	-3.37011	-1.75027
XLOC_000639	NA	-5.39444	-5.67405	-3.32561	-1.81602
XLOC_000640	UNKNOWN	-2.61444	-3.37919	-2.21954	-0.97905
XLOC_000671	circadian locomoter output cycles protein kaput	-1.91452	-2.14428	-0.833905	-1.21212
XLOC_000743	zinc finger protein 423 isoform X1; zinc finger protein 423 isoform X3	-4.02995	-3.72062	-1.68736	-1.8322
XLOC_000847	NA	-3.95118	-3.72324	-3.47435	-2.7494
XLOC_000868	NA	-5.82128	-6.08632	-3.14841	-1.76445
XLOC_001054	polycomb group protein Pc	-2.12822	-2.02307	-1.0904	-1.03436
XLOC_001201	epidermal growth factor receptor-like isoform X1	-1.9969	-1.59446	-0.948602	-1.46299
XLOC_001491	fibrillin-2-like	-1.64312	-1.2683	-1.69808	-1.09211
XLOC_001743	glucose transport transcription regulator RGT1-like isoform X5	-1.00977	-1.40064	-1.2919	-0.87519
XLOC_001854	GK15001	-4.17662	-1.67924	-1.91939	-2.23695
XLOC_001922	NA	-3.9226	-4.65757	-2.87813	-1.95584
XLOC_001923	LOW QUALITY PROTEIN: E3 ubiquitin-protein ligase AMFR-like; NA	-2.82081	-2.76601	-0.944441	-0.83077

XLOC_002082	putative epidermal cell surface receptor-like isoform X3; putative epidermal cell surface receptor-like isoform X4; putative epidermal cell surface receptor-like isoform X1	-1.03207	-1.38118	-1.00006	-1.71345
	intracellular protein transport protein USO1 isoform X9; intracellular protein transport protein USO1 isoformX1; intracellular protein transport protein USO1 isoform X4	-1.29338	-1.39537	-1.4636	-1.00486
XLOC_002126	LOW QUALITY PROTEIN: ATPase family AAA domain-containing protein 2-like; NA	-2.15995	-1.89384	-1.36327	-1.76539
XLOC_002273	uncharacterized protein LOC100883637; protein kibra-like isoformX1; protein kibra-like isoform X3; hemK methyltransferase family member 1-like; protein kibra-like isoformX2	-1.61737	-1.83798	-1.43386	-1.40537
XLOC_002516	NA	-3.91636	-3.73168	-2.29028	-1.99223
XLOC_002641	protein disulfide-isomerase; dynein intermediate chain 2, axonemal-like isoform X1	-1.83521	-2.70821	-1.07176	-1.28419
XLOC_002676	jouberin-like	-2.16729	-3.39501	-1.48141	-1.20838
XLOC_002677	protein kinase DC2 isoform X2	-2.04769	-1.82283	-2.57024	-1.47873
XLOC_002772	protein IWS1 homolog isoform X1; major facilitator superfamily domain-containing protein 6-like; NA	-3.63021	-4.8682	-2.55362	-1.52643
XLOC_002867	Neurabin-1; NA	-1.50576	-1.03405	-0.912184	-1.03677
XLOC_002914	F-box only protein 9-like	-1.20265	-1.72157	-1.15218	-1.51695
XLOC_003020					
XLOC_003076	thiamine transporter 2-like isoform X1	-3.22267	-3.60102	-1.91586	-1.626
XLOC_003372	NA	-3.23201	-3.0219	-2.31105	-0.79977
XLOC_003373	NA	-3.35061	-3.28779	-2.40453	-0.75942
XLOC_003376	hypothetical protein EAI_10632	-4.71774	-3.86827	-2.77322	-1.27842
XLOC_003656	NA	-7.69007	-6.72293	-4.49449	-0.97392
XLOC_003692	xaa-Pro aminopeptidase 1-like	-6.33235	-4.21449	-3.20003	-2.19633
XLOC_003804	oxidative stress-induced growth inhibitor 1-like isoform X3; oxidative stress-induced growth inhibitor 1-like isoform X1	-1.3415	-1.67765	-1.32836	-0.83588
	unknown; uncharacterized protein LOC102670919 isoform X1; uncharacterized protein LOC100884121; PWWP domain-containing protein 2B	-1.71107	-1.83833	-0.841306	-0.99899
XLOC_004156					
XLOC_004357	ornithine decarboxylase-like isoform X2	-1.81331	-1.88967	-0.837024	-0.67539
XLOC_004433	echinoderm microtubule-associated protein-like CG42247-like isoform X1	-4.15721	-3.48029	-1.47681	-1.67896
XLOC_004567	L-lactate dehydrogenase-like isoform X2	-2.67519	-3.79792	-0.770505	-1.84291
XLOC_004792	macoilin-2-like isoform X5; macoilin-2-like isoform X2	-3.27455	-2.7218	-1.12947	-1.57075
XLOC_005103	dehydrogenase/reductase SDR family member 11-like isoform X1	-0.952708	-1.5805	-0.709732	-1.45278
XLOC_005331	fatty acyl-CoA reductase 1-like; histone-lysine N-methyltransferase SETMAR-like protein disabled isoform X2; protein disabled isoform X1	-4.00347	-5.32569	-1.55781	-1.70144
XLOC_005723	NA	-2.99617	-2.69818	-1.91861	-1.33197
XLOC_006007	serine/threonine-protein kinase PAK 3 isoform 1; NA	-2.54307	-2.81	-1.99582	-1.85699
XLOC_006092					
XLOC_006431	AGAP04970-PA-like protein; uncharacterized protein LOC100878076	-4.20318	-1.85051	-2.27102	-1.4857
XLOC_006509	TPA_inf: venus kinase receptor; NA	-2.01728	-2.23549	-0.785111	-0.80492
XLOC_006884	clustered mitochondria protein homolog isoform X2; protein KIAA0664 homolog; NA	-3.15805	-2.43977	-1.03805	-1.51649
XLOC_006935	ATP-binding cassette sub-family A member 2-like isoform X2; tubulin polyglutamylase complex subunit 2-like protein sidekick isoformX2; protein sidekick isoform X6	-4.34923	-4.15524	-1.88717	-2.10146
XLOC_007004					
XLOC_007473	AT-rich interactive domain-containing protein 5B-like isoform X2	-3.72056	-3.33797	-2.0764	-2.37986

XLOC_007474	LIM domain-binding protein 2-like isoform X5; LIM domain-binding protein 2-like isoform X4; LIM domain-binding protein 2-like isoform X1; LIM domain-binding protein 2-like isoform X6; LIM domain-binding protein 2-like isoform X2	-1.57499	-1.63969	-1.26571	-1.15377
XLOC_007698	NA	-3.68325	-3.99231	-1.95958	-1.62642
XLOC_008108	serine protease 53; carboxypeptidase B-like	-3.88872	-5.44181	-2.93231	-4.25817
XLOC_008253	Regulation of nuclear pre-mRNA domain-containing protein	-1.4271	-0.933312	-1.06877	-0.79133
XLOC_008483	solute carrier family 28 member 3-like; solute carrier family 28 member 3-like isoform X1; Protein lozenge; NA	-7.47333	-5.45115	-4.72747	-4.73679
XLOC_008555	inhibin beta chain-like	-3.51061	-3.06489	-3.03947	-1.57125
XLOC_008557	NA	-3.96124	-3.3292	-2.76829	-1.65819
XLOC_008664	kazrin; kazrin-like isoform X1	-1.87128	-1.17187	-1.53011	-1.03332
XLOC_008673	NA	-6.79757	-5.99119	-3.43283	-1.65537
XLOC_008714	leucine-rich repeat extensin-like protein 5	-1.72448	-1.50604	-1.04012	-1.09767
XLOC_008736	uncharacterized protein LOC100882035	-1.31908	-1.71415	-0.959057	-0.88946
XLOC_008762	ankyrin repeat and zinc finger domain-containing protein 1-like isoform X1	-1.46216	-1.4786	-1.22672	-0.71754
XLOC_008924	basement membrane-specific heparan sulfate proteoglycan core protein-like; NA	-0.911436	-1.47412	-1.22645	-0.83703
XLOC_008947	adenomatous polyposis coli protein-like thioredoxin reductase 1 isoform 1; thioredoxin reductase 1 isoform 2;	-1.94194	-2.30214	-1.00662	-1.05562
XLOC_008975	thioredoxin reductase 1 isoform X1	-2.2411	-2.506	-0.98454	-1.12806
XLOC_009015	pro-resilin; NA	-2.20828	-2.98148	-1.96073	-1.30797
XLOC_009039	Transcriptional regulatory protein PHO23; WD repeat-containing protein 66-like cell wall protein AWA1-like isoform X2; zinc finger protein 182-like; NA	-1.90437	-1.96055	-1.15959	-0.83614
XLOC_009164	LOW QUALITY PROTEIN: transcription initiation factor TFIID subunit 4-like	-2.55228	-1.87196	-2.21701	-1.0772
XLOC_009167	actin cytoskeleton-regulatory complex protein PAN1-like; NA	-1.2528	-0.845839	-0.653884	-0.69662
XLOC_009306		-4.53276	-3.43719	-2.91889	-2.29969
XLOC_009453	rab11 family-interacting protein 4-like isoform X3; rab11 family-interacting protein 4-like isoform X2; rab11 family-interacting protein 4-like isoform X1; NA	-1.75306	-1.55894	-0.842513	-0.71387
XLOC_009805	ets DNA-binding protein pokkuri-like isoform X1	-2.40203	-2.45776	-1.02253	-0.9435
XLOC_010064	guanine nucleotide-binding protein G(i) subunit alpha-like	-1.61431	-1.24017	-0.641023	-0.85756
XLOC_010075	AP2-associated protein kinase 1-like isoform X3; NA; AP2-associated protein kinase 1-like isoform X1	-1.5949	-1.33799	-1.06068	-1.26152
XLOC_010098	UDP-glucose 6-dehydrogenase-like isoform X1	-2.40082	-1.67467	-1.06674	-1.30597
XLOC_010166	NA	-1.23168	-2.8134	-1.60595	-0.98826
XLOC_010324	kinesin 12 isoform X1; kinesin 12 isoform X2	-2.4687	-2.16581	-1.30935	-1.2397
XLOC_010426	ubinuclein-1-like isoform X3	-2.13467	-1.96614	-1.27415	-1.04231
XLOC_010483	SH3 domain-containing RING finger protein 3 isoform X2	-2.12276	-1.54819	-0.799758	-0.80918
XLOC_010516	NA	-3.63493	-3.35975	-3.04607	-3.22486
XLOC_010772	hematopoietically-expressed homeobox protein HHEX-like	-2.18888	-1.73119	-1.67187	-1.35052
XLOC_010782	A-kinase anchor protein; NA	-1.76878	-2.37394	-0.950721	-1.19525
XLOC_010940	GATA zinc finger domain-containing protein 14-like isoform X1	-3.83669	-4.09536	-1.52698	-1.90945
XLOC_011061	cadherin-87A-like isoform X2; cadherin-87A-like isoform X1	-1.18714	-1.15907	-1.22606	-1.0473
XLOC_011125	phospholipase DDHD1-like isoform X1	-2.89851	-2.41683	-1.30423	-1.61904
XLOC_011490	cadherin-23-like	-3.14756	-2.28173	-2.01772	-2.70212
XLOC_011887	general transcriptional corepressor trfA-like	-1.1941	-1.14213	-0.609824	-0.64119
XLOC_012539	NA	-1.72836	-1.50702	-1.87866	-1.56017
XLOC_012572	whirlin-like isoform X6; whirlin-like isoform X5; whirlin-like isoform X7	-4.25688	-3.99277	-2.85524	-2.89653
XLOC_012582	brain-specific angiogenesis inhibitor 1-like isoform X2	-2.67731	-3.297	-1.40192	-1.58815

XLOC_012609	ecdysteroid-regulated gene E74 isoform X9; ecdysteroid-regulated gene E74 isoform X10	-1.01903	-1.4378	-1.12468	-1.3119
XLOC_012643	kelch domain-containing protein 10-like; NA; Kelch repeat domain-containing protein KIAA0265-like protein	-2.19634	-2.21591	-0.84165	-0.822
XLOC_012682	autophagy protein 5	-4.44174	-4.20224	-2.22356	-1.60066
XLOC_012953	Protein suppressor of sable histone-lysine N-methyltransferase 2D-like	-3.25238	-2.41475	-0.671817	-0.67389
XLOC_012973	isoform X2	-1.81194	-1.24174	-0.912764	-1.02164
XLOC_012974	histone-lysine N-methyltransferase 2C microtubule-associated protein futsch	-6.08048	-5.07772	-1.32419	-1.16619
XLOC_013024	isoform X3	-1.75735	-1.27341	-0.767125	-2.10526
XLOC_013390	multidrug resistance-associated protein 4-like isoform X5	-3.44656	-3.7396	-0.983117	-1.47107
XLOC_013455	mutS protein homolog 4-like	-2.33049	-2.71405	-1.15721	-1.39518
XLOC_013550	flocculation protein FLO11 isoform X1	-3.67711	-2.06264	-1.5768	-1.23444

November versus March Up Regulated Genes		Fold change			
Gene_ID	Description	ELab	LLab	EField	LField
XLOC_000017	bifunctional ATP-dependent dihydroxyacetone kinase/FAD-AMP lyase (cyclizing)-like	1.50365	1.70879	0.902522	1.74549
XLOC_000116	NA	1.69614	2.11925	2.47806	1.73173
XLOC_000170	transferrin isoform X2; transferrin isoform X1	1.72901	1.79756	1.47638	1.48936
XLOC_000172	putative vacuolar protein sorting-associated protein TDA6-like; odorant binding protein 13 precursor	1.82569	1.26425	0.926072	0.836264
XLOC_000183	Roundabout-like protein	2.75431	1.30461	1.22064	1.70252
XLOC_000209	fibrillin-2-like; fibrillin-1-like; nimrod C2 isoform X5	3.46052	2.33922	1.98428	1.49593
XLOC_000348	LOW QUALITY PROTEIN: cytochrome c oxidase subunit 3-like	1.29027	2.35442	1.66558	1.46976
XLOC_000400	hypothetical protein LOC100646468	1.27063	1.22028	1.05776	1.41615
XLOC_000432	39S ribosomal protein L38, mitochondrial isoform X2	1.30715	1.42954	1.00938	0.935193
XLOC_000750	kinesin 6A isoform X2	1.29475	0.652609	0.704655	0.759243
XLOC_000808	hemolymph lipopolysaccharide-binding protein-like	2.87204	2.15737	1.96199	1.72007
XLOC_000861	GA29194; gag-pol polyprotein precursor; probable sodium/potassium/calcium exchanger CG1090-like; Retrovirus-related Pol polyprotein from transposon 17.6	1.8841	2.41287	1.43934	1.57991
XLOC_000900	LOW QUALITY PROTEIN: homogentisate 1,2-dioxygenase; uncharacterized protein LOC100878942; proto-oncogene tyrosine-protein kinase receptor Ret-like isoform X3 beta-1,4-N-acetylgalactosaminyltransferase bre-4	1.91335	1.45075	1.24333	1.1363
XLOC_000973	isoform X1	1.32632	0.665537	1.23635	1.05251
XLOC_000974	low density lipoprotein receptor adapter protein 1-B-like isoform X1; low density lipoprotein receptor adapter protein 1-B-like isoform X2	1.30719	1.25365	2.06999	1.51145
XLOC_001140	protein GPR107-like isoform X2; protein GPR107-like isoform X1	2.03368	1.95068	1.30015	1.14415
XLOC_001291	apolipoprotein of lipid transfer particle-III; unknown	2.55516	2.52097	0.999428	1.74513
XLOC_001519	NA	0.877949	1.37817	1.28874	0.772334
XLOC_001757	guanine nucleotide exchange factor for Rab-3A-like isoform X5	1.49645	1.55807	2.02369	0.688201
XLOC_001885	probable cytochrome P450 6a14	2.50164	1.51213	1.55979	1.24315
XLOC_002020	dipeptidyl peptidase 3-like isoform 1	1.02069	1.03469	0.797325	0.941222
XLOC_002096	very-long-chain enoyl-CoA reductase-like vacuolar fusion protein MON1 homolog A-like	2.34271	1.92626	1.49978	0.702429
XLOC_002128		1.46861	1.10432	0.859105	1.04562

XLOC_002234	voltage-dependent calcium channel subunit alpha-2/delta-3-like isoform X4;	1.60401	1.7161	1.64443	1.16477
XLOC_002267	voltage-dependent calcium channel subunit alpha-2/delta-3-like isoform X2; scm-like with four MBT domains protein 2-like; voltage-dependent calcium channel subunit alpha-2/delta-3-like isoform X1; voltage-dependent calcium channel subunit alpha-2/delta-3-like isoform X3 phosphoglycolate phosphatase-like	1.22418	1.11837	1.73753	3.00243
XLOC_002394	1,4-alpha-glucan-branching enzyme-like	0.632434	0.628256	1.01848	0.708103
XLOC_002473	beta-galactosidase-like isoform X1	1.69982	1.92783	1.18379	1.65342
XLOC_002510	B-cell receptor-associated protein 31-like organic cation transporter protein-like isoform X1	0.689085	0.935705	1.20993	0.68041
XLOC_002544	probable serine/threonine-protein kinase tsuA-like; poly(U)-specific endoribonuclease homolog	1.48868	1.69124	0.986312	0.891967
XLOC_002633	E3 ubiquitin-protein ligase RNF13-like	1.0323	1.19338	1.04638	1.04769
XLOC_002720	isoform X3	1.16382	1.4514	0.665909	1.15851
XLOC_002803	probable 2-oxoglutarate dehydrogenase E1 component DHKT1 homolog, mitochondrial-like isoform X2	1.48882	1.26853	1.11989	1.24163
XLOC_002909	ATP synthase subunit delta, mitochondrial isoform 3	1.77845	1.0803	1.02075	0.788689
XLOC_002958	hemolymph lipopolysaccharide-binding protein-like	2.87624	3.24502	1.30312	1.12232
XLOC_002965	phospholipase B1, membrane-associated-like isoform X1; phospholipase B1, membrane-associated-like isoform X2; phospholipase B1, membrane-associated-like isoform X3; phospholipase B1, membrane-associated-like; NA; piggyBac transposable element-derived protein 4-like	1.2822	1.14989	1.673	1.58391
XLOC_003039	Protein CBG01525	1.94829	1.25179	0.974401	1.21429
XLOC_003053	NADP-dependent malic enzyme isoform X2; NADP-dependent malic enzyme isoformX1	2.20468	1.93941	0.933031	1.39181
XLOC_003073	tetratricopeptide repeat protein 27-like	1.54362	0.854052	0.896729	0.684391
XLOC_003082	26S proteasome non-ATPase regulatory subunit 1-like	1.70847	2.3377	1.09148	1.55636
XLOC_003104	myophilin	0.901412	1.34867	0.859767	0.63533
XLOC_003407	transaldolase; UDP-galactose translocator; zinc finger protein 330 homolog	0.626347	0.768737	1.18485	0.735647
XLOC_003423	dentin sialophosphoprotein-like	1.38687	1.45197	0.9966	1.53967
XLOC_003594	probable chitinase 2-like	2.62316	2.27683	1.9135	1.51723
XLOC_003700	antitrypsin-like	1.62514	1.40216	1.46173	1.27774
XLOC_003727	protein yellow-like	1.45315	2.06549	1.98923	1.65939
XLOC_003951	Transposable element Tc3 transposase; AAEL004957-PA	2.32098	1.77477	0.939756	0.975128
XLOC_004040	dimethyladenosine transferase 1, mitochondrial	0.781623	0.763038	0.822052	1.08088
XLOC_004157	serine proteinase stubble isoform X3; inhibitor of growth protein 3; serine proteinase stubble isoform X2	1.78774	3.6801	1.09825	1.17625
XLOC_004632	adipokinetic hormone receptor; vacuolar protein sorting-associated protein 37B-like; WAS protein family homolog 1-like	1.0213	1.29354	1.41875	1.07825
XLOC_004664	coiled-coil domain-containing protein 39-like	1.7276	1.05419	1.01268	0.956536
XLOC_004692	putative serine protease K12H4.7-like	1.60191	2.24677	1.35088	1.60539
XLOC_004836	isoform X2	1.67461	1.49233	1.26704	1.95544
XLOC_004853	NA; cytochrome P450 9e2-like	0.852726	0.932697	1.7031	0.883262
XLOC_004872	trehalase-like isoform X3; trehalase-like isoform X2	1.96168	2.03697	1.32663	1.19936
XLOC_005013	transmembrane 7 superfamily member 3-like isoform X2	1.78502	1.65842	1.06829	1.17531
XLOC_005171	uncharacterized protein LOC100875756	1.0112	1.1447	0.836913	0.628139

XLOC_005245	STT3, subunit of the oligosaccharyltransferase complex, homolog B	1.23794	1.33743	1.10552	0.842241
XLOC_005286	enolase-phosphatase E1-like; NA	1.57743	1.29438	1.03455	1.0806
XLOC_005354	lysosomal aspartic protease	1.30771	1.06768	0.841834	0.678833
XLOC_005498	slit homolog 2 protein	2.46266	1.45209	0.906142	2.21633
XLOC_005499	prosaposin isoformX1	1.15919	1.50353	1.61611	1.22729
XLOC_005557	defensin-2 precursor	4.20264	4.75516	3.17195	3.71842
XLOC_005703	Protein CBG22994	3.3524	2.00884	1.98434	1.98708
XLOC_005708	hypothetical protein SINV_02134	1.99551	2.10103	2.31298	1.85039
XLOC_005969	intracellular protein transport protein USO1 isoform X2; intracellular protein transport protein USO1 isoform X3; intracellular protein transport protein	0.6358	0.769531	1.21005	1.24572
XLOC_006082	E3 ubiquitin-protein ligase LRSAM1-like isoform X2; E3 ubiquitin-protein ligase LRSAM1-like isoform X1; E3 ubiquitin-protein ligase LRSAM1-like isoform X3	1.13846	1.40642	0.820937	1.0075
XLOC_006239	CD63 antigen isoform X3 ropporin-1-like protein-like;	1.04611	1.84318	1.36058	1.61607
XLOC_006456	transmembrane protein 132C-like isoform X2; Ropporin-1-like protein	3.07679	2.43847	1.58482	1.70652
XLOC_006480	ATP-dependent RNA helicase DDX42-like isoform X2	1.8849	1.23173	0.739482	1.06486
XLOC_006528	microsomal triglyceride transfer protein large subunit isoform X1; microsomal triglyceride transfer protein large subunit isoform X2	1.6989	0.74555	1.47132	0.717422
XLOC_006557	serine/threonine-protein kinase fused isoform X1	1.40857	1.12571	0.728722	0.585465
XLOC_006618	neuroendocrine convertase 1-like	2.27965	1.42942	1.41255	1.85226
XLOC_006693	uncharacterized transmembrane protein DDB_G0289901-like; cytochrome P450 6A5; hypothetical protein	2.34481	0.810436	1.33376	1.11939
XLOC_006844	NA	2.29657	1.93637	0.988697	0.973896
XLOC_007069	alpha-2-macroglobulin receptor-associated protein-like	1.06145	1.34651	0.9713	0.904445
XLOC_007125	acyl-CoA Delta(11) desaturase-like; acyl-CoA desaturase 1-like	1.51348	1.58093	1.95892	1.35504
XLOC_007577	beat protein, putative; G17145; hypothetical protein V502_03873	2.74371	2.73968	1.4286	1.33746
XLOC_007675	probable cytochrome P450 304a1	1.51264	2.45039	2.51965	2.26726
XLOC_007693	COMM domain-containing protein 4-like	2.44357	1.5611	0.925062	1.91384
XLOC_007706	proteasome subunit alpha type-2 methylglutaryl-CoA hydratase, mitochondrial-like isoform 1	0.670538	1.85662	0.631973	1.18309
XLOC_007772	thyrotropin-releasing hormone receptor-like; cytochrome P450 9e2-like	0.710416	0.862048	1.3232	0.809647
XLOC_007799	NA	2.23402	1.45183	2.16927	1.55999
XLOC_007819	renin receptor-like isoform X3	1.25219	1.38871	0.768567	1.51568
XLOC_008054	peptidoglycan-recognition protein S2 precursor; pyridoxine-5'-phosphate oxidase-like isoform X2; peptidoglycan-recognition protein S2 isoform X1; peptidoglycan-recognition protein LB isoform X1; pyridoxine-5'-phosphate oxidase-like isoform X1	1.50518	1.76169	1.0292	0.645333
XLOC_008127	alcohol dehydrogenase class-3 isoform X2; phosphatidylinositol-glycan biosynthesis class F protein-like	0.919897	1.08268	1.31273	2.20449
XLOC_008170	alkaline phosphatase, tissue-nonspecific isozyme-like isoform X1	1.80707	2.19191	1.33861	2.88108
XLOC_008342	T-complex protein 1 subunit delta-like isoform 1	2.30638	1.97523	1.77136	1.35367
XLOC_008359	solute carrier family 35 member G1-like	1.36898	1.24945	0.7792	0.788414
XLOC_008471	chitinase-like protein Igf4-like isoform X2; chitinase-like protein Igf4-like isoform X1	1.24343	0.912746	1.36664	1.31764
XLOC_008660	sterol O-acyltransferase 1-like	0.968329	0.768328	0.577088	0.591241
XLOC_008763	60S ribosomal protein L11-like	1.38106	1.28955	1.211	0.832413
XLOC_009032	serine/arginine repetitive matrix protein 1-like isoform X1	2.38227	2.4519	1.31092	1.05362
XLOC_009067	NADH dehydrogenase	2.79806	2.53313	1.9634	1.71556
XLOC_009205	60S ribosomal protein L11-like	1.7881	1.41367	1.0435	1.01947
XLOC_009248	serine/arginine repetitive matrix protein 1-like isoform X1	0.951424	1.14887	0.685215	0.757128
XLOC_009257	NADH dehydrogenase	1.1308	0.95325	0.811921	1.21129

XLOC_009270	putative leucine-rich repeat-containing protein DDB_G0290503-like isoform X1; putative leucine-rich repeat-containing protein DDB_G0290503-like isoform X2	1.3828	1.0573	1.35494	0.985919
XLOC_009292	NA	0.977403	0.906172	0.898156	0.929471
XLOC_009303	CD151 antigen isoformX1	0.651443	1.12698	0.690324	1.19125
XLOC_009376	cytochrome P450 9e2	3.38511	3.12983	2.89255	1.51497
XLOC_009817	fructose-1,6-bisphosphatase 1-like isoform X1	3.19996	2.94356	1.52238	1.66606
XLOC_009968	39S ribosomal protein L54, mitochondrial cytochrome c oxidase subunit 4 isoform 1, mitochondrial isoform X1	1.81803	1.96939	1.17471	1.37501
XLOC_009997	LOW QUALITY PROTEIN: ceramide synthase 6	1.48588	0.998534	0.721195	0.947051
XLOC_010014	aquaporin AQPAn.G-like isoform X5	1.92981	0.982425	1.65441	1.66524
XLOC_010287	lymphocyte cytosolic protein 2-like isoform X2; lymphocyte cytosolic protein 2-like isoform X1	1.27238	2.78355	1.6136	1.0617
XLOC_010550	ubiquitin-like domain-containing CTD phosphatase 1-like isoform 1	2.07657	0.781873	1.13293	1.14285
XLOC_010610	trans-1,2-dihydrobenzene-1,2-diol dehydrogenase-like isoformX2	1.87744	1.32488	0.79157	0.903492
XLOC_010624	carboxypeptidase Q-like isoform 1	3.34743	2.37448	1.43242	0.985214
XLOC_010685	prostaglandin reductase 1-like	1.88283	1.74811	0.869291	1.55134
XLOC_010774	NA	1.64745	1.22159	0.728251	0.861131
XLOC_010843	26S protease regulatory subunit 7	1.98626	1.89745	1.54027	1.56765
XLOC_011178	KH domain-containing, RNA-binding, signal transduction-associated protein 3-like isoformX2; KH domain-containing, RNA-binding, signal transduction-associated protein 3-like isoform X4; $\beta$ -galactose dehydrogenase-like isoform X1; NA	0.862812	0.777795	0.66126	0.814379
XLOC_011328	selenoprotein S-like	1.65383	1.22705	0.978352	0.883898
XLOC_011811	phosphoglycerate kinase isoform 1	1.63379	1.53464	1.19466	0.845155
XLOC_011815	peroxisomal biogenesis factor 19-like isoform X2	1.28327	1.23649	0.952739	1.42729
XLOC_011927	codanin-1-like	1.66168	1.72078	0.850193	1.17496
XLOC_011959	slit homolog 2 protein-like	0.863971	1.43053	1.31505	1.04498
XLOC_011978	serine/threonine/tyrosine-interacting protein-like	3.14245	3.07718	2.60638	1.98241
XLOC_012370	transmembrane protein 64-like isoform 1; 26S proteasome non-ATPase regulatory subunit 2	2.36408	2.12438	1.05324	1.60741
XLOC_012528	ABC transporter G family member 20-like; STAM-binding protein-like isoform X1	0.69282	0.665037	0.692864	0.895571
XLOC_012926	cytoplasmic aconitate hydratase-like isoform 1	1.05559	1.26358	1.38641	0.860924
XLOC_012976	dentin sialophosphoprotein-like isoform X1	1.30195	1.34691	0.762615	1.24068
XLOC_013010	extended synaptotagmin-1 isoform X2	1.91898	1.34544	1.03352	0.895341
XLOC_013059	GH11933; GM17678; uncharacterized protein LOC100879727	1.76759	1.70806	1.02474	1.04082
XLOC_013094	CRE-binding bZIP protein SKO1-like	1.48622	1.66671	0.955457	1.94458
XLOC_013342	AAEL014316-PA; uncharacterized protein LOC100875253	2.10034	2.26716	1.73886	1.78568
XLOC_013445		2.67876	2.28028	1.46264	1.82054

## November versus May Down Regulated Genes

Gene_ID	Description	Fold change			
		ELab	LLab	EField	LField
XLOC_001360	inactive tyrosine-protein kinase 7-like Low-density lipoprotein receptor-related protein	-1.90022	-1.30586	-1.49186	-2.41635
XLOC_001548	SCO-spondin	-1.31476	-0.825519	-0.883264	-2.20039
XLOC_001549	fibrillin-1-like	-1.55866	-1.15701	-0.887249	-2.45068
XLOC_002311	Opioid-binding protein/cell adhesion molecule-like protein	-2.58342	-1.71073	-1.57853	-2.4697
XLOC_003459	cuticular protein analogous to peritrophins 3-C precursor; cuticular protein analogous to peritrophins 3-C isoform X1	-2.56543	-2.18593	-1.6385	-1.21054
XLOC_004315	dehydrogenase/reductase SDR family member 11-like isoform X1	-2.03884	-1.91911	-0.846597	-1.55098
XLOC_005103	ATP-dependent RNA helicase WM6-like isoform X2	-2.10864	-2.03807	-1.0722	-1.32061
XLOC_005735		-0.945008	-0.654885	-0.715148	-1.39031

XLOC_005793	hypothetical protein LOC100648478; proton-coupled amino acid transporter 1-like; luciferin 4-monoxygenase; uncharacterized protein LOC102679348;	-1.61061	-1.79777	-0.805202	-1.08085
XLOC_006055	Protein CBG24464 heat shock protein 90	-1.40257	-1.31225	-1.24537	-1.60469
XLOC_006626	probable serine/threonine-protein kinase CG32666-like isoform X4	-1.16344	-2.05834	-1.49793	-1.23628
XLOC_007192	MATH and LRR domain-containing protein PFE0570w-like	-0.762231	-0.72142	-0.704589	-1.52196
XLOC_007219	histone H3-like	-3.4622	-3.65013	-4.66522	-3.54494
XLOC_008665	glutamyl-tRNA(Gln) amidotransferase subunit A, mitochondrial isoform X2	-1.20911	-1.10877	-1.1174	-1.11204
XLOC_008680	probable rRNA-processing protein EBP2 homolog	-1.12266	-0.881733	-0.966935	-1.51568
XLOC_008958	histone-lysine N-methyltransferase SETMAR-like	-1.26487	-0.852147	-0.871285	-0.89969
XLOC_008965	facilitated trehalose transporter Tret1-like	-1.64562	-2.71789	-1.71369	-2.48265
XLOC_009738	nucleolar protein 58-like	-1.81247	-1.81009	-1.32729	-1.48454
XLOC_010064	guanine nucleotide-binding protein G(i) subunit alpha-like	-1.62016	-1.03317	-1.37286	-1.93575
XLOC_010077	S-adenosylmethionine synthase-like isoform X2; S-adenosylmethionine synthase-like isoform X1	-1.32683	-2.66721	-0.938533	-2.58651
XLOC_010282	protein lethal(2)essential for life-like activator of 90 kDa heat shock protein	-2.3665	-2.00483	-4.57975	-3.86023
XLOC_011050	ATPase homolog 1-like isoform 2	-1.25806	-1.52423	-1.64099	-2.10323
XLOC_011171	ribosomal RNA processing protein 1 homolog	-1.24675	-1.10419	-1.15262	-1.57178

## November versus May Up Regulated Genes

Gene_ID	Description	Fold change			
		Elab	Llab	Efield	Lfield
XLOC_000014	p21-activated protein kinase-interacting protein 1-like; mitochondrial enolase superfamily member 1-like	0.791766	1.21509	1.28593	2.00239
XLOC_000170	transferrin isoform X2; transferrin isoform X1	1.64081	1.8106	0.72509	1.38604
XLOC_000178	probable peroxisomal acyl-coenzyme A oxidase 1-like isoform X1 beta-1,4-N-acetylgalactosaminyltransferase bre-4	1.20798	1.16307	1.62987	1.92028
XLOC_000973	isoform X1	0.990811	0.697403	1.32508	1.84728
XLOC_001027	2-acylglycerol O-acyltransferase 1-like isoform X2	2.06307	1.67173	1.39454	2.56701
XLOC_001534	tubulin-specific chaperone cofactor E-like protein-like isoform X5	1.03429	1.30068	1.53473	1.38683
XLOC_001830	endothelin-converting enzyme 1-like isoform X2	1.2642	0.900132	2.46864	4.08365
XLOC_001884	probable cytochrome P450 6a14	2.64119	1.96535	1.79888	1.32792
XLOC_002128	vacuolar fusion protein MON1 homolog A-like	1.37926	1.35333	0.805929	1.60049
XLOC_002234	voltage-dependent calcium channel subunit alpha-2/delta-3-like isoform X4; voltage-dependent calcium channel subunit alpha-2/delta-3-like isoform X2; scm-like with four MBT domains protein 2-like; voltage-dependent calcium channel subunit alpha-2/delta-3-like isoform X1; voltage-dependent calcium channel subunit alpha-2/delta-3-like isoform X3	2.28446	1.74261	2.69412	3.13865
XLOC_002267	phosphoglycolate phosphatase-like insulin-like growth factor-binding protein complex acid labile subunit-like isoform X6; NA histone demethylase UTY-like	1.77116	2.26048	2.22424	4.69938
XLOC_002464	Gag-Pol polyprotein; putative gag-pol protein; gag-pol polyprotein; retrovirus-related Pol polyprotein from transposon	1.10564	1.92096	1.40608	2.55601
XLOC_002606	412	1.85651	1.57419	2.95324	2.61206
XLOC_003207	DNA-dependent protein kinase catalytic subunit-like	1.25585	0.888782	0.659827	0.77809
XLOC_003688	antitrypsin-like	1.93975	2.42888	0.882101	1.08853
XLOC_003700	protein yellow-like	1.34754	1.71332	0.993686	2.12871
XLOC_003727	NA	2.46811	1.92622	1.45353	1.56375
XLOC_004576	probable cytochrome P450 6a14	1.50129	1.71511	1.38009	1.16094
XLOC_004644	trehalase-like isoform X3; trehalase-like isoform X2	2.96651	1.8562	2.04158	1.31375
XLOC_004853		1.43586	0.807289	1.24873	2.55595

XLOC_005178	LOW QUALITY PROTEIN: synaptogyrin-2	0.977541	0.640635	0.879847	0.630424
XLOC_005708	hypothetical protein SINV_02134	1.13011	1.86932	0.872083	2.02979
	intracellular protein transport protein				
	USO1 isoform X2; intracellular protein				
	transport protein USO1 isoform X3;				
	intracellular protein transport protein				
XLOC_005969	USO1 isoform X1	0.943718	0.758028	1.07773	1.89201
	succinyl-CoA ligase; B-cell CLL/lymphoma 6				
	member B protein-like isoform X3; broad-				
	complex core protein isoforms 1/2/3/4/5-				
	like; probable succinyl-CoA ligase; zinc				
XLOC_006244	finger and BTB domain-containing protein				
XLOC_006826	12-like isoform X3	0.863026	1.37112	1.08654	0.997324
	filamin-like	1.07386	0.788336	0.966519	0.669447
XLOC_007125	acyl-CoA Delta(11) desaturase-like; acyl-				
	CoA desaturase 1-like	1.5447	1.53842	1.09331	2.32417
	membrane metallo-endopeptidase-like 1-				
	like isoform X1; membrane metallo-				
	endopeptidase-like 1-like isoform X2;				
	membrane metallo-endopeptidase-like 1-				
XLOC_007157	like isoform X4	2.51037	1.84952	3.798	5.12476
	G-protein coupled receptor Mth2; G-				
XLOC_007364	protein coupled receptor Mth2-like	1.07175	0.759531	1.51537	2.1259
XLOC_007675	probable cytochrome P450 304a1	2.42562	2.60989	1.0459	0.794614
XLOC_007772	methylglutaconyl-CoA hydratase,				
XLOC_008342	mitochondrial-like isoform 1	1.49088	1.09299	1.26372	1.50372
	vitellogenin precursor	2.61617	2.19515	2.54016	4.40232
XLOC_008471	alkaline phosphatase, tissue-nonspecific				
XLOC_008559	isozyme-like isoform X1	1.22741	0.912605	1.3442	1.47756
	growth/differentiation factor 8-like	1.14805	0.835426	0.595997	1.28722
	DNA-directed RNA polymerase II subunit				
	RPB1-like isoform X2; endothelin-				
	converting enzyme 1 isoformX1;				
	endothelin-converting enzyme 1 isoform				
XLOC_008560	X3	1.53937	0.925303	1.10121	0.757176
XLOC_008880	AAEL009939-PA; NA	1.94053	2.71347	1.92468	2.72487
XLOC_009067	sterol O-acyltransferase 1-like	3.20971	3.19117	1.15553	1.32291
XLOC_009292	NA	1.44461	1.82984	1.07876	2.58231
XLOC_009328	leucine-rich repeat and immunoglobulin-				
	like domain-containing nogo receptor-				
	interacting protein 2-like isoform X2				
		0.922541	1.05426	1.61726	1.20681
XLOC_009487	thiolester-containing protein 7 isoform X2	2.26295	2.23399	1.51511	0.831849
XLOC_009817	fructose-1,6-bisphosphatase 1-like isoform				
	X1	2.76334	3.17643	0.634717	0.847193
XLOC_009976	putative ferric-chelate reductase 1				
	homolog isoformX1; putative ferric-				
	chelate reductase 1 homolog isoform X2	1.00011	1.10697	1.40651	1.25712
	LOW QUALITY PROTEIN: ceramide				
XLOC_010014	synthase 6	2.72583	1.9941	1.69546	2.45966
XLOC_010222	trichohyalin	0.889642	1.00615	1.30878	1.53044
XLOC_010287	aquaporin AQPAn.G-like isoform X5	1.17866	2.65865	0.745425	1.02177
XLOC_010475	mediator of RNA polymerase II				
XLOC_010824	transcription subunit 1-like isoform X1	1.12444	1.6583	2.13945	1.94443
	Protein CBG24896	1.48349	1.27777	2.97786	1.84461
XLOC_011150	ring canal kelch homolog isoform X1; ring				
XLOC_012381	canal kelch homolog isoform X2	1.3227	1.20599	1.6071	0.971226
XLOC_012475	NA	2.39558	3.30194	2.03118	3.44214
XLOC_012854	Neuroligin-4, X-linked	2.75022	2.31759	1.26803	1.56411
	galactosylgalactosylxylosylprotein 3-beta-				
	glucuronosyltransferase I	0.986492	1.34939	0.624251	0.753575
XLOC_012926	ABC transporter G family member 20-like;				
	STAM-binding protein-like isoform X1	1.0226	1.14958	1.2322	1.05378

## January versus March Down Regulated Genes

Gene_ID	Description	Fold change			
		ELab	LLab	EField	LField

XLOC_001255	membrane-associated guanylate kinase, WW and PDZ domain-containing protein 2 isoform X6; membrane-associated guanylate kinase, WW and PDZ domain-containing protein 2 isoform X3;	-1.61277	-0.866413	-0.721585	-0.67016
XLOC_005153	membrane-associated guanylate kinase, WW and PDZ domain-containing protein 2 isoform X4; membrane-associated guanylate kinase, WW and PDZ domain-containing protein 2 isoform X5	-1.62244	-0.851872	-1.23555	-0.92814
XLOC_005723	interaptin-like	-0.925606	-0.950133	-1.12607	-1.23173
XLOC_006277	zinc finger protein 800-like isoform X3	-2.07711	-1.47051	-1.36621	-1.21407
XLOC_009202	translational activator GCN1-like	-0.785683	-0.751714	-0.878482	-0.74848
XLOC_009686	hyccin-like isoform X2	-2.39825	-1.45709	-0.98077	-1.52478
XLOC_010635	probable G-protein coupled receptor 125-like	-2.12821	-1.14714	-1.54789	-1.24454
XLOC_010745	scavenger receptor class B member 1 isoform X5; scavenger receptor class B member 1 isoform X2	-1.88711	-0.962065	-0.727644	-0.7829

January versus March Up Regulated Genes		Fold change			
Gene_ID	Description	ELab	LLab	EField	LField
XLOC_000017	bifunctional ATP-dependent dihydroxyacetone kinase/FAD-AMP lyase (cyclizing)-like	1.41951	1.55999	0.841941	1.35272
XLOC_000176	protein brown; transcriptional regulator ATRX homolog	1.03909	0.701954	0.625806	0.919161
XLOC_000183	Roundabout-like protein fibrillin-2-like; fibrillin-1-like; nimrod C2	1.9434	1.13037	1.16451	1.97119
XLOC_000209	isoform X5	2.8817	0.621235	1.84942	1.36406
XLOC_000900	LOW QUALITY PROTEIN: homogentisate 1,2-dioxygenase; uncharacterized protein LOC100878942; proto-oncogene tyrosine-protein kinase receptor Ret-like isoform X3	1.15831	1.0252	1.58047	1.20692
XLOC_000974	low density lipoprotein receptor adapter protein 1-B-like isoform X1; low density lipoprotein receptor adapter protein 1-B-like isoform X2	1.6386	1.18947	1.60785	1.74119
XLOC_001207	peptidyl-prolyl cis-trans isomerase FKB14-like	0.991592	1.3063	0.952865	1.21951
XLOC_001326	putative fatty acyl-CoA reductase CG5065-like	1.47661	1.05012	1.08408	1.40717
XLOC_001361	homeobox protein OTX1 A-like isoform X1	0.761825	0.797405	1.33192	1.04588
XLOC_001366	sodium-coupled monocarboxylate transporter 2-like isoform X2; heat shock protein 83-like; integrin-alpha FG-GAP repeat-containing protein 2-like	1.32754	1.26	1.24359	1.38375
XLOC_001523	BMP-binding endothelial regulator protein isoform X1; BMP-binding endothelial regulator protein isoform X2	1.27288	0.906537	1.37752	1.62667
XLOC_001568	dynactin subunit 5	1.33149	0.73484	0.73526	0.914417
XLOC_001627	NA	2.82881	2.26495	2.42639	1.9307
XLOC_001757	guanine nucleotide exchange factor for Rab-3A-like isoform X5	1.20547	0.758421	1.87246	0.841967
XLOC_002009	gamma-interferon-inducible-lysosomal thiol reductase-like	1.25902	1.20575	1.45448	1.04823
XLOC_002098	cysteine-rich protein 2-binding protein-like	0.895182	0.945923	1.39774	0.879549
XLOC_002128	vacuolar fusion protein MON1 homolog A-like	1.46984	0.705956	0.800758	1.01362
XLOC_002234	voltage-dependent calcium channel subunit alpha-2/delta-3-like isoform X4; voltage-dependent calcium channel subunit alpha-2/delta-3-like isoform X2; scm-like with four MBT domains protein 2-like; voltage-dependent calcium channel subunit alpha-2/delta-3-like isoform X1; voltage-dependent calcium channel subunit alpha-2/delta-3-like isoform X3	1.01318	1.39851	1.17505	1.19138
XLOC_002267	phosphoglycolate phosphatase-like	0.945737	0.920559	1.64732	3.52755

XLOC_003053	NADP-dependent malic enzyme isoform X2; NADP-dependent malic enzyme				
XLOC_003370	isoformX1	1.90831	1.06576	1.12935	1.0513
XLOC_003423	Ac1147-like protein	0.838523	3.20974	1.46495	4.02074
XLOC_003700	dentin sialophosphoprotein-like	1.31922	1.13787	0.821117	1.27788
XLOC_003727	antitrypsin-like	1.45375	0.881096	1.07136	1.40184
XLOC_004087	protein yellow-like	0.705252	1.09662	0.97582	1.57722
	transferrin 1 precursor	1.47562	1.51247	1.09871	1.6443
XLOC_004486	uncharacterized protein LOC100865969	1.01525	2.93248	1.91902	3.4455
XLOC_004539	dipeptidase 1 isoform X1	1.07571	0.876752	1.24849	0.683222
XLOC_004541	ND5_10414 NADH dehydrogenase subunit	2.21077	1.05245	1.45665	0.682477
XLOC_004576	5 (mitochondrion)	1.09358	1.30796	1.04431	1.5382
XLOC_004760	NA	2.31586	1.72222	1.45436	2.09564
	hexamerin 70c precursor				
XLOC_004872	transmembrane 7 superfamily member 3-				
XLOC_005067	like isoform X2	1.09762	1.18656	0.788574	1.12613
XLOC_005354	Ac1147	1.01311	2.84544	1.35601	3.92667
XLOC_005499	lysosomal aspartic protease	1.22092	0.600234	0.648211	1.09302
	prosaposin isoformX1	0.929184	0.701646	0.974615	1.26117
XLOC_005541	hemolymph lipopolysaccharide-binding				
XLOC_005557	protein-like	1.55571	1.27921	1.395	0.59693
XLOC_005708	defensin-2 precursor	3.79765	3.92365	3.41796	6.00043
XLOC_005847	hypothetical protein SINV_02134	1.00077	1.2738	1.39496	1.71455
	NA	1.58593	2.37477	1.88103	2.64538
XLOC_005848	mushroom body large-type Kenyon cell-specific protein 1; mushroom body large-type Kenyon cell-specific protein 1 isoform				
XLOC_006239	X2	0.751695	1.68926	1.06063	1.69207
	CD63 antigen isoform X3	0.593359	0.830673	1.0773	1.53884
	armadillo segment polarity protein				
XLOC_006415	isoform X2; armadillo segment polarity protein isoform X1; atrial natriuretic peptide-converting enzyme isoform X3;				
	armadillo segment polarity protein				
	isoform X6	1.09925	0.587985	0.599717	0.798458
XLOC_006480	ATP-dependent RNA helicase DDX42-like				
	isoform X2	1.3668	0.890433	0.837625	1.13262
XLOC_006690	probable cytochrome P450 6a17 isoform 1	0.820608	1.16	0.950872	1.18153
XLOC_006713	probable methylmalonate-semialdehyde dehydrogenase	0.763061	0.610649	0.660891	0.933476
XLOC_007077	organic cation transporter protein-like				
	isoform 1	1.02452	0.859868	1.59056	1.12489
XLOC_007125	acyl-CoA Delta(11) desaturase-like; acyl-CoA desaturase 1-like				
	muscle segmentation homeobox-like				
XLOC_007303	isoform X2	1.22861	1.1864	0.928819	1.44125
XLOC_007577	beat protein, putative; GI17145; hypothetical protein V502_03873	1.98497	1.51771	1.7679	1.77322
	protein unc-13 homolog D isoform X1;				
	protein unc-13 homolog D isoform X2;				
	protein unc-13 homolog D isoform X5;				
XLOC_007579	protein unc-13 homolog D isoform X4	1.57857	0.670217	0.884513	1.0872
XLOC_007675	probable cytochrome P450 304a1	1.73431	1.76274	1.81639	2.58504
XLOC_007819	NA	1.92082	2.11572	1.82158	2.53648
XLOC_007820	steroid receptor seven-up, isoforms B/C				
XLOC_007963	endochitinase isoform 2	1.42765	0.803084	1.05376	0.970877
XLOC_008054	renin receptor-like isoform X3	2.09832	0.871682	1.40133	1.04832
XLOC_008097	fumarylacetocetase	1.27522	0.881174	0.838171	0.756495
XLOC_008121	protein hairy isoform X2	1.61115	1.22044	0.824676	1.10194
XLOC_008170	cysteine dioxygenase type 1-like	1.61104	2.0685	0.816999	1.4034
	uncharacterized protein LOC100877842;				
	GPI ethanolamine phosphate transferase 3-				
XLOC_008192	like	1.66847	1.51991	1.48626	2.05543
XLOC_008342	vitellogenin precursor	1.97504	2.60964	2.40973	3.02311
XLOC_008350	vitellogenin precursor	1.76845	1.27831	1.41267	2.37754
	alkaline phosphatase, tissue-nonspecific				
XLOC_008471	isozyme-like isoform X1	2.38095	1.18508	1.82801	2.77871
XLOC_008889	golgin subfamily B member 1-like	1.39991	1.16766	0.975362	1.35938
		1.44763	0.908157	1.20712	1.66686
XLOC_009032	chitinase-like protein Igf4-like isoform X2;				
XLOC_009067	chitinase-like protein Igf4-like isoform X1	1.85888	1.63711	0.711915	1.03
XLOC_009205	sterol O-acyltransferase 1-like	0.918358	1.14655	1.37318	2.47802
	60S ribosomal protein L11-like	1.86816	0.892499	0.684829	0.810672
	putative leucine-rich repeat-containing				
	protein DDB_G0290503-like isoform X1;				
	putative leucine-rich repeat-containing				
XLOC_009270	protein DDB_G0290503-like isoform X2	1.09688	0.677408	0.954814	1.27352
XLOC_009292	NA	0.835717	0.884022	0.746291	1.07181
XLOC_009303	CD151 antigen isoformX1	1.39891	1.03949	0.788087	1.52541

XLOC_009321	MOSC domain-containing protein 2, mitochondrial-like serine--pyruvate aminotransferase, mitochondrial-like isoform X3	1.04293	0.999788	1.0189	1.37446
XLOC_009565	fructose-1,6-bisphosphatase 1-like isoform	0.881754	0.955233	1.19174	1.14257
XLOC_009817	X1	2.381	1.738	0.752525	2.32804
XLOC_009968	39S ribosomal protein L54, mitochondrial	1.42133	1.36968	1.01979	1.14189
XLOC_010166	NA	0.958475	3.15908	1.10439	3.01654
XLOC_010274	PDZ domain-containing protein 2	1.38531	0.866463	1.58444	1.96442
XLOC_010350	cathepsin J-like; growth/differentiation factor 8-like isoform 1; acidic fibroblast growth factor intracellular-binding protein isoform X1	1.07722	0.860573	1.44283	1.05411
XLOC_010568	fumarylacetoacetate hydrolase domain-containing protein 2A-like isoform X2	1.2924	0.835384	0.733897	1.01863
XLOC_010751	AAEL009036-PA	3.37036	1.82004	2.32483	2.18877
XLOC_010853	uncharacterized protein LOC101742759	0.730094	2.8699	1.46885	3.5197
XLOC_011328	KH domain-containing, RNA-binding, signal transduction-associated protein 3-like isoform X2; KH domain-containing, RNA-binding, signal transduction-associated protein 3-like isoform X4; L-galactose dehydrogenase-like isoform X1; NA	1.03175	0.618475	0.845812	0.95171
XLOC_011815	phosphoglycerate kinase isoform 1 nuclelease-sensitive element-binding protein 1 isoform X4	1.02411	0.876288	0.790059	0.590985
XLOC_011934	codonin-1-like	0.708047	0.820409	0.710339	0.921235
XLOC_011959	slit homolog 2 protein-like	1.02449	0.675187	1.00613	1.19718
XLOC_011978	proteasome subunit alpha type-3; pteropsin; pteropsin isoform X3	1.86516	1.49144	1.66294	1.16732
XLOC_012402	Neuroligin-4, X-linked	0.737508	0.61075	0.632747	0.716276
XLOC_012475	beta-hexosaminidase subunit beta-like	1.96059	0.879703	1.52764	1.67243
XLOC_012490	ABC transporter G family member 20-like; STAM-binding protein-like isoform X1	2.15086	1.0727	1.31414	1.88101
XLOC_012926	dentin sialophosphoprotein-like isoform	0.782884	0.642779	0.777486	1.08303
XLOC_013010	X1	1.58744	1.07745	0.855386	0.971525
XLOC_013123	ecdysone-induced protein 75 isoform X3; ecdysone-induced protein 75 isoform X5; ecdysone-induced protein 75 isoform X4	1.90034	1.66165	1.5478	1.83204
XLOC_013126	ecdysone-induced protein 75 isoform X5	1.95898	0.939259	1.0013	0.79437
XLOC_013167	UDP-glucuronosyltransferase 1-3-like	1.47056	0.733568	1.38802	1.01189
XLOC_013225	nidogen-2	1.51011	0.720936	1.25468	0.869909
XLOC_013445	AAEL014316-PA; uncharacterized protein LOC100875253	2.0008	1.51592	1.71789	1.40761

## January versus May Down Regulated Genes

Gene_ID	Description	Fold change			
		ELab	LLab	EField	LField
XLOC_001416	bifunctional glutamate/proline-tRNA ligase	-1.04332	-1.3317	-0.999877	-1.61993
XLOC_004318	probable chitinase 3	-4.40005	-2.01013	-1.41526	-4.76728
XLOC_007845	RNA-binding protein 28-like	-0.867674	-1.04555	-1.21233	-1.63172
XLOC_009160	calpain-C isoform X1; calpain-C isoform X2; vesicle transport protein GOT1B-like isoform 2	-1.38705	-1.37168	-1.9682	-1.27741
XLOC_009738	nucleolar protein 58-like	-1.58215	-1.68464	-0.912098	-1.81266
XLOC_012148	pre-mRNA-splicing factor CWC22 homolog; NA	-1.08432	-1.3601	-1.00654	-0.84581
XLOC_012638	box C/D snoRNA protein 1-like	-1.22343	-1.69507	-1.15831	-2.02248

## January versus May Up Regulated Genes

Gene_ID	Description	ELab	LLab	EField	LField
XLOC_000176	protein brown; transcriptional regulator ATRX homolog	1.1053	0.792152	1.13563	2.35314
XLOC_000178	probable peroxisomal acyl-coenzyme A oxidase 1-like isoform X1	0.895407	1.09744	1.32312	2.2767
XLOC_001534	tubulin-specific chaperone cofactor E-like	0.797487	0.609452	1.346	1.68199
XLOC_001884	protein-like isoform X5	2.48714	1.61142	1.47891	1.18093
XLOC_002128	probable cytochrome P450 6a14	1.3805	0.954961	0.747582	1.56849
	vacuolar fusion protein MON1 homolog A-like				

XLOC_002218	Zinc finger BED domain-containing protein; Monocarboxylate transporter 12; monocarboxylate transporter 12 isoform X2	0.644759	0.783395	1.3362	1.21713
XLOC_002234	voltage-dependent calcium channel subunit alpha-2/delta-3-like isoform X4;	1.69362	1.42501	2.22474	3.16526
XLOC_002267	voltage-dependent calcium channel subunit alpha-2/delta-3-like isoform X2; scm-like with four MBT domains protein 2- like; voltage-dependent calcium channel subunit alpha-2/delta-3-like isoform X1;	1.49272	2.06268	2.13403	5.2245
XLOC_002464	voltage-dependent calcium channel subunit alpha-2/delta-3-like isoform X3	1.17501	1.95019	1.64501	2.51057
XLOC_002606	phosphoglycolate phosphatase-like	1.33244	1.45855	2.19318	2.33897
XLOC_003080	insulin-like growth factor-binding protein complex acid labili subunit-like isoform X6; NA	0.630181	0.602329	2.07898	1.32246
XLOC_003681	histone demethylase UTY-like antithrombin-III zinc finger MIZ domain-containing protein 1	1.56158	0.761564	2.81215	2.12679
XLOC_004099	GTP-binding protein RIT2 isoform X4; ras- related protein Rap-2a; ras-related and estrogen-regulated growth inhibitor-like isoform X3	1.3299	0.864092	1.12979	1.3126
XLOC_004576	NA	0.983629	1.3019	1.9416	1.41983
XLOC_004644	probable cytochrome P450 6a14 AGAP003453-PA-like protein; AAELO09899-	2.72312	1.63506	1.49205	1.29852
XLOC_004976	PA	2.05924	2.25279	3.00167	3.57347
XLOC_005263	succinate dehydrogenase	0.894122	0.958776	0.581728	1.12683
XLOC_005847	NA	1.6384	0.876837	2.48286	2.45019
XLOC_005848	mushroom body large-type Kenyon cell- specific protein 1; mushroom body large- type Kenyon cell-specific protein 1 isoform X2	1.13207	0.809616	2.31078	2.73015
XLOC_005969	intracellular protein transport protein USO1 isoform X2; intracellular protein transport protein USO1 isoform X3; intracellular protein transport protein USO1 isoform X1	0.629295	0.624087	0.622941	1.21427
XLOC_006244	succinyl-CoA ligase; B-cell CLL/lymphoma 6 member B protein-like isoform X3; broad- complex core protein isoforms 1/2/3/4/5- like; probable succinyl-CoA ligase; zinc finger and BTB domain-containing protein 12-like isoform X3	0.833082	1.11141	0.906326	1.31725
XLOC_006361	integrin alpha-PS2 isoform X1; integrin alpha-PS2 isoform X2	0.910792	1.02891	3.19522	3.79161
XLOC_006742	carbonic anhydrase 2-like	1.24966	0.994175	0.618641	0.81557
XLOC_007077	organic cation transporter protein-like isoform 1	1.77569	1.04327	3.39398	3.03126
XLOC_007157	membrane metallo-endopeptidase-like 1- like isoform X1; membrane metallo- endopeptidase-like 1-like isoform X2; membrane metallo-endopeptidase-like 1- like isoform X4	1.69394	1.4741	3.6877	4.10849
XLOC_007364	G-protein coupled receptor Mth2; G- protein coupled receptor Mth2-like	1.21293	0.803423	1.25205	2.47694
XLOC_007772	methylglutaconyl-CoA hydratase, mitochondrial-like isoform 1	1.26606	0.730897	1.28923	1.82756
XLOC_007819	NA	1.3432	1.42072	1.6913	1.48057
XLOC_007820	steroid receptor seven-up, isoforms B/C	1.43155	0.931339	1.69485	1.84464
XLOC_008342	vitellogenin precursor	2.07824	1.49823	2.18147	5.42619
XLOC_008471	alkaline phosphatase, tissue-nonspecific isozyme-like isoform X1	1.38389	1.16752	0.952923	1.5193
XLOC_008559	growth/differentiation factor 8-like DNA-directed RNA polymerase II subunit RPB1-like isoform X2; endothelin- converting enzyme 1 isoform X1; endothelin-converting enzyme 1 isoform X3	1.31303	1.11119	1.08009	1.59568
XLOC_008560	leucine-rich repeat and immunoglobulin- like domain-containing nogo receptor- interacting protein 2-like isoform X2	1.65969	0.942291	1.36334	1.15451
XLOC_008889	golgin subfamily B member 1-like	1.39994	1.66664	0.781531	3.6824
XLOC_009292	NA	1.30292	1.80769	0.926898	2.72465
XLOC_009328	LOW QUALITY PROTEIN: ceramide synthase 6	1.59827	1.70805	1.74569	2.2091
XLOC_010014		1.27256	1.30313	0.920489	2.29214

XLOC_010274	PDZ domain-containing protein 2	0.896087	1.00655	1.05502	0.845656
XLOC_010475	mediator of RNA polymerase II transcription subunit 1-like isoform X1 metalloproteinase inhibitor 3-like isoform	0.863	1.58879	1.58317	2.25789
XLOC_010822	X1	1.81469	1.0506	1.16159	2.40959
XLOC_010824	Protein CBG24896	1.83461	1.50907	1.93508	2.68494
XLOC_011224	protein apterous isoform X1; protein apterous isoform X2	1.02555	0.948123	1.43361	1.77912
XLOC_011314	synapse-associated protein of 47 kDa-like isoform X1	0.745036	0.676415	0.980766	1.69014
XLOC_011621	zinc finger protein Noc-like synaptotagmin 20 isoform X5; synaptotagmin 20 isoform X1	0.94533	0.781827	1.4712	0.75964
XLOC_011972		1.71437	1.12154	1.31397	2.2516
XLOC_012027	integrator complex subunit 1-like isoform X1; nuclear RNA export factor 2-like	0.751439	1.09507	1.48114	0.866904
XLOC_012035	Dystroglycan	0.941008	0.706131	0.990278	1.79588
XLOC_012381	NA	0.98789	2.17493	2.20378	3.84416
XLOC_012467	1-phosphatidylinositol 4,5-bisphosphate phosphodiesterase	0.725253	0.736105	0.873634	1.75389
XLOC_012475	Neuroligin-4, X-linked	2.45047	1.36152	1.06828	2.9161
XLOC_013123	ecdysone-induced protein 75 isoform X3; ecdysone-induced protein 75 isoform X5; ecdysone-induced protein 75 isoform X4	1.70621	1.89961	1.59901	1.75257
XLOC_013126	ecdysone-induced protein 75 isoform X5	1.68083	1.67121	1.08859	1.68165
XLOC_013167	UDP-glucuronosyltransferase 1-3-like 5-oxoprolinase-like isoform X3; 5-oxoprolinase-like isoform X1	1.05767	1.02251	2.15815	1.30765
XLOC_013174		0.901583	0.7131	0.892409	0.599241

## March versus May Down Regulated Genes

Gene_ID	Description	Fold change			
		ELab	LLab	EField	LField
XLOC_003732	nucleoporin GLE1-like 116 kDa U5 small nuclear ribonucleoprotein component-like isoform	-1.36212	-1.24333	-2.17715	-1.84799
XLOC_006461	1	-0.775048	-0.838976	-0.784269	-1.41868
XLOC_007192	MATH and LRR domain-containing protein PFE0570w-like	-0.595953	-0.639069	-1.05324	-1.16976
XLOC_007706	proteasome subunit alpha type-2 26S proteasome non-ATPase regulatory	-0.777346	-0.829726	-2.27769	-1.77344
XLOC_010171	subunit 1-like cuticular protein analogous to peritrophins	-0.71211	-0.735978	-1.65168	-1.15444
XLOC_010272	3-B precursor	-1.30325	-1.01395	-2.44432	-0.82548
XLOC_013090	cytochrome P450 4C1	-0.974106	-1.14314	-1.34765	-3.64508

## March versus May Up Regulated Genes

Gene_ID	Description	Fold change			
		ELab	LLab	EField	LField
XLOC_002606	histone demethylase UTY-like rootletin-like isoform X2; rootletin-like isoform X3	1.31054	0.907654	2.06649	2.29756
XLOC_005010	Reticulocyte-binding protein 2-like protein a	1.51026	1.0801	1.74778	1.43796
XLOC_005139	segmentation protein Runt-like inhibin beta chain-like	0.978907	0.861014	1.51333	1.71158
XLOC_008498	cytochrome b561 domain-containing	0.856666	2.41928	5.15982	6.56997
XLOC_008555	protein 1-like	0.911704	1.31276	4.15919	1.06123
XLOC_010110	metalloproteinase inhibitor 3-like isoform	1.12414	1.30916	2.18881	1.24341
XLOC_010822	X1	0.832648	0.65199	1.0403	1.80593

## November field versus laboratory differentially regulated genes

Gene_ID	Description	Upregulated
XLOC_005574	acetyl-CoA carboxylase-like isoform X9	Field
XLOC_011487	Atherin	Field
	ATP-binding cassette sub-family G member 1	Field
XLOC_008193	AT-rich interactive domain-containing protein 5B-like isoform X2	Field
XLOC_007472	BAG domain-containing protein Samui-like isoform X1	Field
XLOC_000736	biglycan-like	Field
XLOC_001570		Field
XLOC_010350	cathepsin J-like; growth/differentiation factor 8-like isoform 1	Field
XLOC_009023	cell wall protein IFF6-like isoform X1	Field
XLOC_001890	choline-phosphate cytidylyltransferase A-like isoform X4	Field
XLOC_010691	Cytochrome c-2	Field

XLOC_012946	cytosolic purine 5'-nucleotidase-like isoform X3	Field
XLOC_004369	dentin sialophosphoprotein-like isoformX1	Field
XLOC_013147	dnaJ homolog subfamily C member 3	Field
XLOC_011896	elongation of very long chain fatty acids protein	Field
XLOC_009805	ets DNA-binding protein pokkuri-like isoform X1	Field
XLOC_003140	eukaryotic translation initiation factor 4 gamma	Field
XLOC_005611	fatty-acid amide hydrolase 2-like	Field
XLOC_006055	heat shock protein 90	Field
XLOC_012615	heat shock protein cognate 3 precursor	Field
XLOC_008743	heat shock protein cognate 5	Field
XLOC_000143	heat shock protein Hsp70Ab-like	Field
XLOC_003966	HIG1 domain family member 1B-like	Field
	high affinity cAMP-specific and IBMX-insensitive 3',5'-cyclic phosphodiesterase	
XLOC_011377	8A-like	Field
XLOC_004604	homeobox protein caupolicana-like isoform X2	Field
XLOC_009686	hyccin-like isoform X2	Field
	interferon regulatory factor 2-binding	
XLOC_002657	protein-like B-like	Field
XLOC_006619	IP21807p; CG10513	Field
XLOC_009505	JNK-interacting protein 1 isoform X1	Field
XLOC_002677	jouberin-like	Field
	lateral signaling target protein 2 homolog;	
XLOC_004532	NA	Field
XLOC_005452	LIM and SH3 domain protein Lasp-like	Field
	LOW QUALITY PROTEIN: d-2-hydroxyglutarate dehydrogenase,	
XLOC_001384	mitochondrial-like	Field
	LOW QUALITY PROTEIN: E3 ubiquitin-protein ligase AMFR-like	
XLOC_001923	MAP kinase-interacting serine/threonine-protein kinase 2	Field
XLOC_011937	MLX-interacting protein isoform X3	Field
XLOC_001107	moesin/ezrin/radixin homolog 1 isoform X12	Field
XLOC_010073	mucin-19-like isoform X1	Field
XLOC_012310	NAD kinase-like isoform X3	Field
XLOC_008480	NF-kappa-B inhibitor cactus 1	Field
XLOC_000531	nicotinate phosphoribosyltransferase-like isoformX1	Field
XLOC_002622	nuclear distribution protein nudE-like 1-A-like isoform X3	Field
XLOC_001098	organic cation transporter protein-like isoform 1	Field
XLOC_007077	periaxin-like	Field
XLOC_007013	PHD finger protein 20-like isoform X2	Field
XLOC_011161	phosphatase and actin regulator 4 isoform X5	Field
XLOC_006978		
XLOC_012308	phosphatidylinositol 4-kinase beta-like	Field
	polypeptide N-acetylgalactosaminyltransferase 5-like; NA	
XLOC_001112		Field
XLOC_000910	protein bicaudal C homolog 1-B isoform X4	Field
XLOC_005808	Protein CBG23823; NA	Field
XLOC_002678	protein disulfide-isomerase TMX3-like isoform X1	Field
	protein kinase C and casein kinase substrate in neurons protein 2-like isoform X6	
XLOC_012170	protein split ends-like	Field
XLOC_006905	Protein suppressor of sable protein TIS11-like	Field
XLOC_012953		
XLOC_006721	protein tyrosine phosphatase type IVA 1 putative fatty acyl-CoA reductase	Field
XLOC_002653	rapulator complex protein LAMTOR1-like	Field
XLOC_005533	rap1 GTPase-activating protein 1 isoform X8	Field
XLOC_009262	ribosomal protein S6 kinase alpha-5 isoform X5	Field
XLOC_010694	scavenger receptor class B member 1 isoform X5	Field
XLOC_007439		
XLOC_010745		Field

XLOC_008752	SEC23-interacting protein-like isoform X1	Field
XLOC_001366	sodium-coupled monocarboxylate	
XLOC_008975	transporter 2-like isoform X2	Field
	thioredoxin reductase 1 isoform 1	Field
XLOC_000430	ubiquitin carboxyl-terminal hydrolase 31-	
XLOC_013167	like isoform 1	Field
XLOC_007658	UDP-glucuronosyltransferase 1-3-like	Field
	uncharacterized serine-rich protein	
XLOC_008056	C215.13-like isoform X1	Field
	WD repeat-containing protein 48 homolog	
	isoform X11	Field
	116 kDa U5 small nuclear	
	ribonucleoprotein component-like isoform	
XLOC_006461	1	Labortory
XLOC_005453	3-hydroxyisobutyrate dehydrogenase,	
XLOC_011131	mitochondrial-like isoform X4	Labortory
	40S ribosomal protein S19a-like	Labortory
XLOC_007289	actin-binding LIM protein 2-like isoform X7	Labortory
XLOC_008436	aminomethyltransferase, mitochondrial-	Labortory
	like	
XLOC_012602	anaphase-promoting complex subunit 15-	Labortory
XLOC_007856	like	Labortory
XLOC_010685	carbohydrate sulfotransferase 11-like	Labortory
	carboxypeptidase Q-like isoform 1	Labortory
XLOC_007710	cyclin-dependent kinase 1-like isoform 1	Labortory
	delta(3,5)-Delta(2,4)-dienoyl-CoA	
XLOC_002395	isomerase	Labortory
XLOC_001568	dynactin subunit 5	Labortory
	fibrillin-2-like; fibrillin-1-like; nimrod C2	
XLOC_000209	isoform X5	Labortory
	galactose-1-phosphate uridylyltransferase-	
XLOC_003439	like	Labortory
XLOC_005056	glutathione S-transferase D1 isoform X5	Labortory
XLOC_002958	hemolymph lipopolysaccharide-binding	Labortory
	protein-like	Labortory
XLOC_000533	histone acetyltransferase KAT7 isoform X1	Labortory
XLOC_005883	homeodomain-only protein-like	Labortory
	lysine-specific histone demethylase 1A	
XLOC_002782	isoform X1	Labortory
	muscle M-line assembly protein unc-89-	
XLOC_009923	like	Labortory
	myosin-1-like isoform X2; myosin-1-like	
XLOC_005665	isoform X3	Labortory
XLOC_013225	nidogen-2	Labortory
	pancreatic triacylglycerol lipase-like	
XLOC_009135	isoform X1	Labortory
	poly(U)-binding-splicing factor half pint	
XLOC_004122	isoform X2	Labortory
XLOC_009983	probable cleavage and polyadenylation	
	specificity factor subunit 2 isoform X1	Labortory
	probable glutamine-dependent NAD(+)	
XLOC_004970	synthetase-like isoform X1	Labortory
XLOC_010835	Protein CBG23823	Labortory
XLOC_010896	protein SMGB-like	Labortory
XLOC_001050	protein snail homolog Sna-like	Labortory
	putative GTP-binding protein 6-like	
XLOC_003543	isoform X1	Labortory
XLOC_008699	quinone oxidoreductase-like protein 2-like	Labortory
XLOC_006456	ropparin-1-like protein-like	Labortory
XLOC_003323	selenocysteine Se-methyltransferase-like	Labortory
XLOC_004157	inhibitor of growth protein 3	Labortory
XLOC_005134	serine/threonine-protein kinase phg2-like	Labortory
	serine/threonine-protein kinase ULK3-like	
XLOC_012179	isoform X4	Labortory
XLOC_002227	spindle pole body component 110-like	Labortory
XLOC_004402	troponin C type I isoform X1	Labortory
XLOC_011080	uncharacterized protein LOC100872724	Labortory
XLOC_000338	UNKNOWN	Labortory
XLOC_010020	zinc transporter ZIP1-like	Labortory

Table S3. Core genes from the between month comparisons common to more than one comparisons; candidate toolkit genes

Gene_ID	Description	Count	November versus	January	March	November versus	May	January versus	March	January versus	May	March versus May
XLOC_000017	bifunctional ATP-dependent dihydroxyacetone kinase/FAD-AMP lyase (cyclizing)-like	2			Up					Up		
XLOC_000170	transferrin isoform X2; transferrin isoform X1	2			Up		Up					
XLOC_000176	protein brown; transcriptional regulator ATRX homolog	2								Up		Up
XLOC_000178	probable peroxisomal acyl-coenzyme A oxidase 1-like isoform X1	2					Up			Up		Up
XLOC_000183	Roundabout-like protein	2			Up					Up		
XLOC_000209	fibrillin-2-like; fibrillin-1-like; nimrod C2 isoform X5	2			Up					Up		
XLOC_000319	NA	2	Down		Down							
XLOC_000445	NA	2	Down		Down							
XLOC_000638	NA	2	Down		Down							
XLOC_000639	NA	2	Down		Down							
XLOC_000640	UNKNOWN	2	Down		Down							
XLOC_000671	circadian locomoter output cycles protein kaput	2	Down		Down							
XLOC_000868	NA	2	Down		Down							
	LOW QUALITY PROTEIN: homogentisate 1,2-dioxygenase; uncharacterized protein LOC100878942; proto-oncogene tyrosine-protein kinase receptor											
XLOC_000900	Ret-like isoform X3	2			Up					Up		
XLOC_000973	beta-1,4-N-acetylgalactosaminyltransferase bre-4 isoform X1	2			Up		Up					
	low density lipoprotein receptor adapter protein 1-B-like isoform X1; low density lipoprotein receptor adapter protein 1-B-like isoform X2					Up				Up		
XLOC_000974	inactive tyrosine-protein kinase 7-like	2	Down					Down				
XLOC_001360												
XLOC_001534	tubulin-specific chaperone cofactor E-like protein-like isoform X5	2					Up				Up	
XLOC_001757	guanine nucleotide exchange factor for Rab-3A-like isoform X5	2				Up				Up		
XLOC_001884	probable cytochrome P450 6a14	2					Up				Up	
XLOC_002082	putative epidermal cell surface receptor-like isoform X3; putative epidermal cell surface receptor-like isoform X4; putative epidermal cell surface receptor-like isoform X1	2	Down		Down							
XLOC_002464	insulin-like growth factor-binding protein complex acid labile subunit-like isoform X6; NA	2						Up			Up	
	uncharacterized protein LOC100883637; protein kibra-like isoform X1; protein kibra-like isoform X3; hemK methyltransferase family member 1-like; protein kibra-like isoform X2											
XLOC_002516	E3 ubiquitin-protein ligase RNF13-like isoform X3	2	Down		Down							
XLOC_002720	NADP-dependent malic enzyme isoform X2; NADP-dependent malic enzyme isoform X1	2	Up		Up							
XLOC_003053	Ac1147-like protein	2	Down		Up						Up	
XLOC_003370	dentin sialophosphoprotein-like	2	Down		Up						Up	
XLOC_003423	NA	2	Down		Down						Up	
XLOC_003656	DNA-dependent protein kinase catalytic subunit-like	2	Up		Up							
XLOC_003688	xa-Pro aminopeptidase 1-like	2	Down		Down							
XLOC_003692	oxidative stress-induced growth inhibitor 1-like isoform X3; oxidative stress-induced growth inhibitor 1-like isoform X1	2	Down		Down							
XLOC_003804	unknown; uncharacterized protein LOC102670919 isoform X1; uncharacterized protein LOC100884121; PWWP domain-containing protein 2B	2	Down		Down							
XLOC_004156	uncharacterized protein LOC100865969	2	Down		Down						Up	
XLOC_004486	probable cytochrome P450 6a14	2	Up		Up						Up	
XLOC_004644	trehalase-like isoform X3; trehalase-like isoform X2	2	Up		Up						Up	
XLOC_004853	transmembrane 7 superfamily member 3-like isoform X2	2	Up		Up						Up	
XLOC_004872	rootletin-like isoform X2; rootletin-like isoform X3	2	Down		Up							
XLOC_005010	Ac1147	2	Down		Down							Up
XLOC_005067	lysosomal aspartic protease	2	Down		Up							
XLOC_005354	prosaposin isoform X1	2	Down		Up							
XLOC_005499	defensin-2 precursor	2	Down		Up							
XLOC_005557	protein disabled isoform X2; protein disabled isoform X1	2	Down		Down						Down	
XLOC_005723	NA	2									Up	
XLOC_005847	mushroom body large-type Kenyon cell-specific protein 1; mushroom body large-type Kenyon cell-specific protein 1 isoform X2	2	Down		Up							
XLOC_005848	heat shock protein 90	2	Down		Up		Down			Up		Up
XLOC_006055	CD63 antigen isoform X3	2										
XLOC_006239	succinyl-CoA ligase; B-cell CLL/lymphoma 6 member B protein-like isoform X3; broad-complex core protein isoforms 1/2/3/4/5-like; probable succinyl-CoA ligase; zinc finger and BTB domain-containing protein 12-like isoform X3	2	Down		Up							
XLOC_006244	ATP-dependent RNA helicase DDX42-like isoform X2	2					Up					
XLOC_006480	ATP-binding cassette sub-family A member 2-like isoform X2; tubulin polyglutamylase complex subunit 2-like	2					Up					
XLOC_006935	organic cation transporter protein-like isoform 1	2	Down		Down							
XLOC_007077	membrane metallo-endopeptidase-like 1-like isoform X1, X2, and X4	2	Up		Up							
XLOC_007157	membrane metallo-endopeptidase-like 1-like isoform X2; membrane metallo-endopeptidase-like 1-like isoform X4	2					Up					
XLOC_007192	MATH and LRR domain-containing protein PFE0570w-like	2					Up					Down
XLOC_007364	G-protein coupled receptor Mth2; G-protein coupled receptor Mth2-like AT-rich interactive domain-containing protein 5B-like isoform X2	2	Down		Down			Up				
XLOC_007473	LIM domain-binding protein 2-like isoform X5; LIM domain-binding protein 2-like isoform X4; LIM domain-binding protein 2-like isoform X1; LIM domain-binding protein 2-like isoform X6; LIM domain-binding protein 2-like isoform X2	2	Down		Down							
XLOC_007474												
XLOC_007577	beat protein, putative; GI17145; hypothetical protein V502_03873	2	Down		Up							
XLOC_007706	proteasome subunit alpha type-2	2	Up		Up							Down
XLOC_007820	steroid receptor seven-up, isoforms B/C	2										
XLOC_008054	renin receptor-like isoform X3	2										
XLOC_008108	serine protease 53; carboxypeptidase B-like	2	Down		Down							
XLOC_008170	cysteine dioxygenase type 1-like	2	Up		Up							
XLOC_008483	solute carrier family 28 member 3-like; solute carrier family 28 member 3-like isoform X1; Protein lozenge; NA	2	Down		Down							
XLOC_008555	inhibin beta chain-like	2	Down		Down							
XLOC_008559	growth/differentiation factor 8-like	2						Up				
	DNA-directed RNA polymerase II subunit RPB1-like isoform X2; endothelin-converting enzyme 1 isoform X1; endothelin-converting enzyme 1 isoform											
XLOC_008560	X3	2						Up				
XLOC_008673	NA	2	Down		Down							
XLOC_008736	uncharacterized protein LOC100882035	2	Down		Down							
XLOC_008889	golgin subfamily B member 1-like	2	Down		Down							
XLOC_008947	adenomatous polyposis coli protein-like	2	Down		Down							
XLOC_009032	chitinase-like protein Idgf4-like isoform X2; chitinase-like protein Idgf4-like isoform X1	2										
XLOC_009164	cell wall protein AWA1-like isoform X2; zinc finger protein 182-like; NA	2	Down		Down							
XLOC_009205	60S ribosomal protein L11-like	2	Up		Up							
	putative leucine-rich repeat-containing protein DDB_G0290503-like isoform X1; putative leucine-rich repeat-containing protein											
XLOC_009270	DDB_G0290503-like isoform X2	2										
XLOC_009303	CD151 antigen isoform X1	2										
XLOC_009306	actin cytoskeleton-regulatory complex protein PAN1-like; NA	2	Down		Down							
XLOC_009328	leucine-rich repeat and immunoglobulin-like domain-containing nogo receptor-interacting protein 2-like isoform X2	2										

XLOC_009453	rab11 family-interacting protein 4-like isoform X3; rab11 family-interacting protein 4-like isoform X2; rab11 family-interacting protein 4-like isoform X1; NA	2	Down	Down	Down		Down
XLOC_009738	nucleolar protein 58-like	2					
XLOC_009805	ets DNA-binding protein pokkuri-like isoform X1	2	Down	Down			
XLOC_009968	39S ribosomal protein L54, mitochondrial	2	Up			Up	
XLOC_010064	guanine nucleotide-binding protein G(i) subunit alpha-like	2	Down	Down	Down		
	AP2-associated protein kinase 1-like isoform X3; NA; AP2-associated protein kinase 1-like isoform X1	2	Down	Down			
XLOC_010075	PDZ domain-containing protein 2	2		Up		Up	Up
XLOC_010274	aquaporin AQPAn.G-like isoform X5	2		Up	Up		
XLOC_010287							
XLOC_010475	mediator of RNA polymerase II transcription subunit 1-like isoform X1	2			Up		Up
XLOC_010822	metalloproteinase inhibitor 3-like isoform X1	2			Up	Up	Up
XLOC_010824	Protein CBG24896	2			Up		
XLOC_010853	uncharacterized protein LOC101742759	2	Down			Up	
XLOC_011050	activator of 90 kDa heat shock protein ATPase homolog 1-like isoform 2 KH domain-containing, RNA-binding, signal transduction-associated protein 3-like isoform X2; KH domain-containing, RNA-binding, signal transduction-associated protein 3-like isoform X4; L-galactose dehydrogenase-like isoform X1; NA	2	Down		Down		
XLOC_011328	cadherin-23-like	2	Down	Up		Up	
XLOC_011490	phosphoglycerate kinase isoform 1	2		Up		Up	
XLOC_011815	general transcriptional corepressor trfA-like	2	Down	Down			
XLOC_011887	cordanin-1-like	2		Up		Up	
XLOC_011959	NA	2			Up		Up
XLOC_012381							
XLOC_012572	whirlin-like isoform X6; whirlin-like isoform X5; whirlin-like isoform X7	2	Down	Down			
XLOC_012582	brain-specific angiogenesis inhibitor 1-like isoform X2	2	Down	Down			
	ecdysteroid-regulated gene E74 isoform X9; ecdysteroid-regulated gene E74 isoform X10	2	Down	Down			
XLOC_012609	autophagy protein 5	2	Down	Down			
XLOC_012682	histone-lysine N-methyltransferase 2C	2	Down	Down			
XLOC_012974	dentin sialophosphoprotein-like isoform X1	2		Up		Up	
XLOC_013010	ecdysone-induced protein 75 isoform X3; ecdysone-induced protein 75 isoform X5; ecdysone-induced protein 75 isoform X4	2				Up	
XLOC_013123	ecdysone-induced protein 75 isoform X5	2				Up	Up
XLOC_013126	UDP-glucuronosyltransferase 1-3-like	2				Up	Up
XLOC_013167	CRE-binding bZIP protein SKO1-like	2	Up	Up		Up	Up
XLOC_013342	AAEL014316-PA; uncharacterized protein LOC100875253	2		Up		Up	
XLOC_002606	histone demethylase UTY-like	3			Up		Up
XLOC_003700	antitrypsin-like	3		Up	Up	Up	
XLOC_003727	protein yellow-like	3		Up	Up	Up	
XLOC_004576	NA	3		Up	Up	Up	Up
XLOC_005103	dehydrogenase/reductase SDR family member 11-like isoform X1	3	Down	Down	Down		
XLOC_005708	hypothetical protein SINV_02134	3		Up	Up	Up	
	intracellular protein transport protein USO1 isoform X2; intracellular protein transport protein USO1 isoform X3; intracellular protein transport protein USO1 isoform X1	3					
XLOC_005969	acyl-CoA Delta(11) desaturase-like; acyl-CoA desaturase 1-like	3		Up	Up		Up
XLOC_007125	probable cytochrome P450 304a1	3		Up	Up	Up	
XLOC_007675	methylglutaconyl-CoA hydratase, mitochondrial-like isoform 1	3		Up	Up		Up
XLOC_007772	NA	3		Up	Up		
XLOC_007819	sterol O-acyltransferase 1-like	3		Up	Up	Up	Up
XLOC_009067	fructose-1,6-bisphosphatase 1-like isoform X1	3		Up	Up	Up	
XLOC_009817	LOW QUALITY PROTEIN: ceramide synthase 6	3		Up	Up		
XLOC_010014	NA	3		Up	Up		Up
XLOC_010166	slit homolog 2 protein-like	3	Down	Down		Up	
XLOC_011978	Neuroligin-4, X-linked	3	Up	Up		Up	Up
XLOC_012475	ABC transporter G family member 20-like; STAM-binding protein-like isoform X1	3			Up	Up	Up
XLOC_012926	vacuolar fusion protein MON1 homolog A-like	4		Up	Up	Up	Up
	voltage-dependent calcium channel subunit alpha-2/delta-3-like isoform X4; voltage-dependent calcium channel subunit alpha-2/delta-3-like isoform X2; scm-like with four MBT domains protein 2-like; voltage-dependent calcium channel subunit alpha-2/delta-3-like isoform X1; voltage-dependent calcium channel subunit alpha-2/delta-3-like isoform X3	4					
XLOC_002234	phosphoglycolate phosphatase-like	4		Up	Up	Up	Up
XLOC_002267	vitellogenin precursor	4		Up	Up	Up	Up
XLOC_008342	alkaline phosphatase, tissue-nonspecific isozyme-like isoform X1	4		Up	Up	Up	Up
XLOC_008471	NA	4		Up	Up	Up	Up
XLOC_009292							

Table S4. Overrepresented Gene Ontology terms and KEGG Pathways within the gene set contributing to the formation of supercluster 1 in the hierarchical cluster analysis<sup>1</sup>

Category	Gene Ontology terms					Ontology <sup>2</sup>
	Over represented pvalue	Under represented pvalue	Number of genes in comparison	Total number of genes in data set	Terms	
GO:0006119	1.95E-09	1	11	16	oxidative phosphorylation	BP
GO:0006412	9.11E-08	1	24	96	translation	BP
GO:0015986	3.50E-07	1	7	9	ATP synthesis coupled proton transport	BP
GO:0042254	4.11E-07	0.9999999	25	109	ribosome biogenesis	BP
GO:0015992	2.74E-06	0.9999997	11	28	proton transport	BP
GO:0006118	3.62E-05	0.9999924	14	50	obsolete electron transport	BP
GO:0006446	2.15E-04	0.9999718	8	21	regulation of translational initiation	BP
GO:0005840	1.34E-12	1	33	107	ribosome	CC
GO:0005737	5.09E-05	0.9999809	29	156	cytoplasm	CC
GO:0045285	1.06E-04	0.9999985	4	5	respiratory chain complex III	CC
GO:0019773	1.94E-04	0.9999967	4	5	proteasome core complex, alpha-subunit complex	CC
GO:0003735	2.57E-07	0.9999999	23	94	structural constituent of ribosome	MF
GO:0046961	1.97E-05	0.9999993	6	9	proton-translocating ATPase activity, rotational mechanism	MF
GO:0004298	5.53E-05	0.9999972	6	10	threonine-type endopeptidase activity	MF
GO:0008121	1.06E-04	0.9999985	4	5	ubiquinol-cytochrome-c reductase activity	MF
GO:0046933	1.60E-04	0.9999974	4	5	proton-translocating ATP synthase activity, rotational mechanism	MF
GO:0003743	2.15E-04	0.9999718	8	21	translation initiation factor activity	MF
KEGG Pathways						
Category	Over represented pvalue	Under represented pvalue	Number of genes in comparison	Total number of genes in data set	Pathway name	
ko00190	2.06E-13	1	35	72	Oxidative phosphorylation	
ko03050	6.81E-05	0.99999	12	25	Proteasome	
ko03010	5.85E-04	0.99979	21	79	Ribosome	

<sup>1</sup>See Figure 4B<sup>2</sup>Ontology abbreviations: Biological processes; BP, Cellular component; CC, Molecular function; MF